EXPERIMENTAL AND THEORETICAL ANALYSIS OF SAFETY-DEGRADATION INTERACTION IN LITHIUM-ION CELLS

A Thesis

by

NEHA KHUSHAL GADA

Submitted to the Office of Graduate and Professional Studies of
Texas A&M University
in partial fulfillment of the requirements for the degree of

MASTER OF SCIENCE

Chair of Committee,	Partha P. Mukherjee
Committee Members,	Waruna Kulatilaka
	Sarbajit Banerjee
Head of Department,	Andreas Polycarpou

May 2017

Major Subject: Mechanical Engineering

ABSTRACT

Lithium ion batteries are quite ubiquitous in terms of their market spread. They represent an extremely compact energy storage device. In addition to making them a lucrative choice for a diverse set of applications, this high energy density and larger terminal voltage also make them quite dangerous if not handled properly. In extreme events, they can also catch fire. To ensure continuous and safe operation, cell manufacturers specify a voltage window of operation. This voltage window describes the lowest discharge voltage and highest charge voltage. Intuitively speaking, the cell stability should not be specified just in terms of one voltage value. Rather, it should be a function of cell temperature as well as charging current. In order to gain insights into the cell operation during and after overcharge, commercial 18650 cells were used for electrochemical cycling. Three major sets of tests were performed on these to answer the following questions: 1) How do Li-ion cells behave if the electrochemical window is manipulated? 2) How does the charging rate affect the overcharge behavior of these cells? 3) Finally, is there a way to track changes occurring during each state of overcharge and perhaps, elucidate the reactions in the cell contributing to overcharge? The results showed that even if the upper voltage limit of Li-ion cells is extended and a higher capacity is gained, the cycle life of the cell diminishes considerably. Secondly, as expected, the charging rate is found to have a significant effect, leading to the hypothesis that overcharge of Li-ion cell is not solely dependent on the upper voltage limit, but also on the charging rate (current). Based on destructive physical analysis (DPA) and electrochemical impedance

spectroscopy measurements, the resistance from the cell separator was found to be a leading presence during overcharge of the cell. Finally, based on overcharge tests and the supporting DPA analysis, it was concurred that overcharge is a cathode dependent process as opposed to the popular belief of anodic dependence.

DEDICATION

Find that one person who serves as a rock, as an emotional anchor to guide you through all the difficult days. Surely, people can be successful by themselves. However, I do believe that success is just that much sweeter when you are able to share it with someone. I am tremendously lucky to be able to call not one, but several people in my life as my rocks; but above all, stand my parents.

This is for them.

ACKNOWLEDGEMENTS

I would like to thank my committee chair, Dr. Partha Mukherjee, and my committee members, Dr. Sarbajit Banerjee and Dr. Waruna Kulatilaka for their guidance and support throughout the course of this research.

Thanks also go to my friends and colleagues at the Energy and Transport Sciences Laboratory and the department staff of Mechanical Engineering at Texas A&M University.

CONTRIBUTORS AND FUNDING SOURCES

This work was supervised by Dr. Partha Mukherjee as the thesis committee chair. Dr. Waruna Kulatilaka of the Department of Mechanical Engineering and Dr. Sarbajit Banerjee of the Department of Chemistry were thesis committee members. All other work conducted for this thesis was completed by the student independently.

This research was supported in part by the faculty research initiation grant from Texas A&M University.

TABLE OF CONTENTS

LIST OF FIGURES

Page

LIST OF TABLES

Page

CHAPTER I

INTRODUCTION

Energy Scope

The outlook for energy use worldwide presented in the International Energy Outlook 2016 (IEO2016) continues to show rising levels of demand over the next three decades [1]. Economic growth along with the accompanying structural changes, strongly influence the world energy consumption. As countries develop and standard of living continues to improve, the demand for energy rises at an ever-growing pace. The world started by harnessing the energy of fossil fuels and that still remains the major source powering all sectors of industry and commerce today. However, a rising awareness towards the need to shift away from fossil fuels as the primary energy source prevails today. The masses have begun to recognize the problems associated with the persistent use of non-renewable energy sources. Because anthropogenic emissions of carbon dioxide (CO_2) result primarily from the combustion of fossil fuels, energy consumption is at the center of the climate change and global warming debate [2]. In the International Energy Outlook 2016 reference case, world energy related CO_2 emissions increase from 32.3 billion metric tons in 2012 to 35.6 billion metric tons in 2020 and to 43.2 billion metric tons in 2040 [1]. This statistic drives home the imminent necessity of finding alternatives to non-renewable energy sources. The scientific community has certainly responded well to this predicament by diving headfirst into several areas of research for finding clean energy sources. Among the possible alternatives, energy sources such as solar and wind have proven to be the most promising. However, as sophisticated

methods for harnessing energy continue to be developed, there are some limitations of these sources that cannot be overcome.

Energy Storage

When it comes to harnessing the power from wind and solar sources, even the best technologies are at the mercy of nature. The production of energy from them does not happen at a continuous rate. There is a significant mismatch between the supply and demand due to the sporadic nature of these energy sources. The nature of demand for energy sources is also not constant. The need for energy is significantly reduced during certain hours of night and very heightened during peak day times. This is where electrochemical energy storage and conversion systems become germane. The energy produced in excess of demand during low-demand periods (night time) can be stored and utilized for subsequent use during periods where there is a deficit of supply in conjunction with excess of demand (peak daytime hours). There are several devices that can be used for electrochemical storage such as flywheels, ultra-capacitors, and compressed air [3].

One of the most prominent devices that distinguish themselves from the rest is batteries. Batteries are capable of storing energy in a way that is convenient, clean and most importantly, safe. The most attractive factor of batteries is their sheer versatility; they can be used for small-scale applications such as portable electronics, or scaled up applications such as EVs and HEVs or for very large scale applications such as in the energy grid. The electrification of passenger vehicles has increasingly become a part of decarbonization conversations in energy policy and business. Prior to 2010,

Energy Information Administration (EIA) estimated a total of 57,000 EVs in use. Between 2010 and 2015, EV sales surpassed 400,000 vehicles with a value of $15 billion. As long as current trends of increasing consumer interest and decreasing costs continue, EV adoption could increase to 12 million vehicles by 2025 [4].

Table 1 Advantages and disadvantages of using Li-ion batteries as energy storage devices.

Advantages	Limitations
Self-contained power source	High cost
Adaptable to user configuration	Use of critical materials
Portability	Low energy density (compared to fuels)
Efficient energy-storage device	Limited shelf life
Ease of availability	
Reliable, low maintenance	
Minimum, if any, moving parts	

Batteries function as backups during the lull in energy production from solar and wind energy. On a day to day basis, batteries are found in almost every device – laptops, cameras, telephone, electronic personal care devices such as toothbrushes, razors, medical devices such as pacemakers, hearing aids, pagers, toys, watches, transportation

applications such as satellites, submarines, and electric and hybrid electric vehicles as previously mentioned. Therefore, energy storage and batteries especially, have become an indispensable alternative to the energy derived from conventional coal, oil and gas. By this point, it has been established that batteries have an indubitably significant role and they can only become even more ubiquitous from here on. Even though the merits of battery energy storage have been highlighted, the fact remains that the high cost, low cycle life and certain safety issues for scaled up applications hinder their widespread implementation in replacement of fossil fuels. The next few sections will summarize the basic working principle of electrochemical cells and the evolution of various battery technologies leading up to the most advanced technology as it stands today.

Battery Energy Storage

Electrochemical sources have certain advantages over other types of energy. As is already discussed, electrochemical energy sources can be used in order to offset the intermittency that is inevitable from solar and wind energy sources. Other sources such as thermal energy are not as clean as electrochemical energy and also involve certain intermediate steps. Thus, electrochemical energy exhibits higher efficiency as compared to other technologies.

An Italian physicist named Alessandro Volta built his first ‘voltaic pile’. This crude battery consisted of paired copper zinc disks separated from one another by cardboard disks saturated with salt or acid solution. The voltaic pile was able to produce continuous electricity and stable current, although his early models could not produce sparks – what we call high voltage cells today. A few years later, John F. Daniell, an

English chemist, developed a way to improve the efficiency of Volta's cells by finding a solution to the corrosion problems. Thus, in 1836, the first Daniell cell was invented. This cell consisted of a zinc electrode immersed in a zinc sulfate solution and a copper electrode immersed in its respective copper sulfate solution. These electrodes were separated by a porous membrane. This membrane allowed the ions to pass but kept the two solutions from mixing with each other. Although laden with problems of its own, the Daniell cell shown in Figure 1 was the first real breakthrough in electrochemistry with its relatively safe, non-corrosive characteristics and an operating voltage of 1.1 V [1].

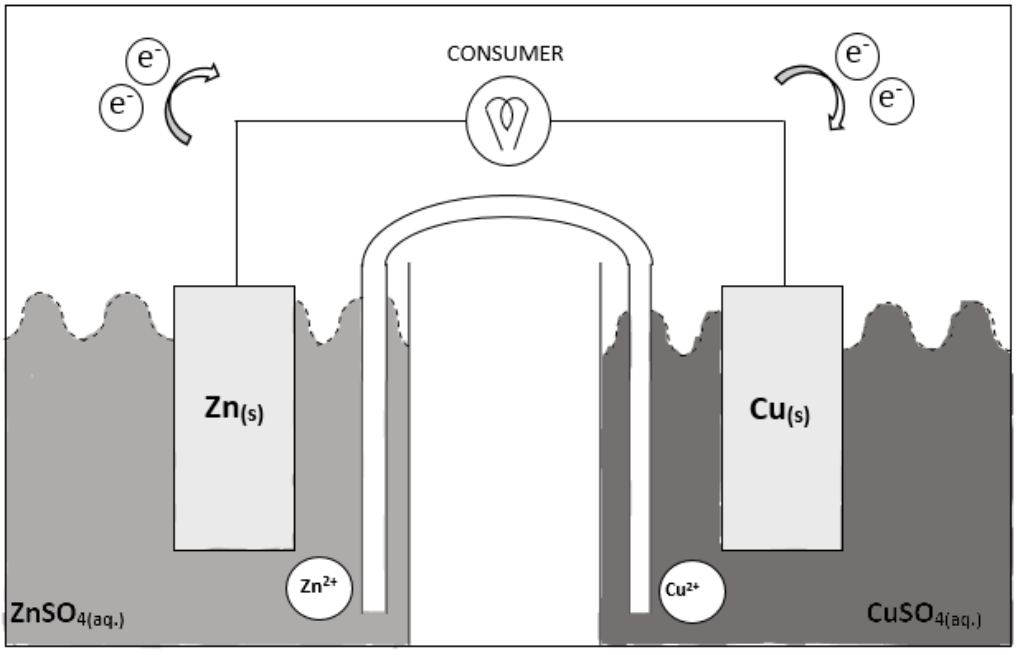

Figure 1 Schematic of the Daniell cell invented by John F. Daniell in 1836.

At this stage, it is important to highlight a distinguishing feature of these cells. Until the 1850s, all the discoveries and improvements made were based off the Voltaic pile and the Daniell cell. When the materials in these cells would be depleted, so would the ability of the cell to produce current. Today, these types of cells are what we refer to as primary cells. Therefore, depending on the principle of operation, cells can be classified as follows:

Primary Cells

These cells are also known as non-rechargeable cells. They are called as such because the electrochemical reaction taking place in the cells is irreversible. There is a fixed amount of reactive material available inside of these cells and once that is exhausted, no more current can be drawn from the cell. Thus, the cell cannot be reused again and is known as a primary cell to depict the fact that these types of cells were discovered in the early years before more sophisticated chemistries and technologies replaced them. A well-known primary cell is the Daniell cell as described previously [5].

Secondary Cells

These are the cells that are used most commonly today. Secondary cells are rechargeable cells; the electrochemical reactions occurring inside the cell are reversible. After the cell is discharged, an externally applied electrical energy (current) forces a reversal of the electrochemical process; as a consequence, the reactants are restored to their original form and the stored energy can be reused [5]. Depending on the lifetime of the battery, this process can be repeated numerous times. This is the fundamental difference and focal advantage of secondary cells over their primary counterparts. There are other

classes of storage devices such as fuel cells, redox flow batteries, supercapacitors which are in the same vein as traditional batteries with a few distinguishing characteristics.

Ideally, batteries should have high energy specific energy and high capacities combined with a compact design. While primary batteries are certainly capable of achieving these deliverables, economic considerations steered the direction of research towards secondary batteries. The working principle of a typical electrochemical cell shown in Figure 2 and the functions of various cell components are discussed in the upcoming section.

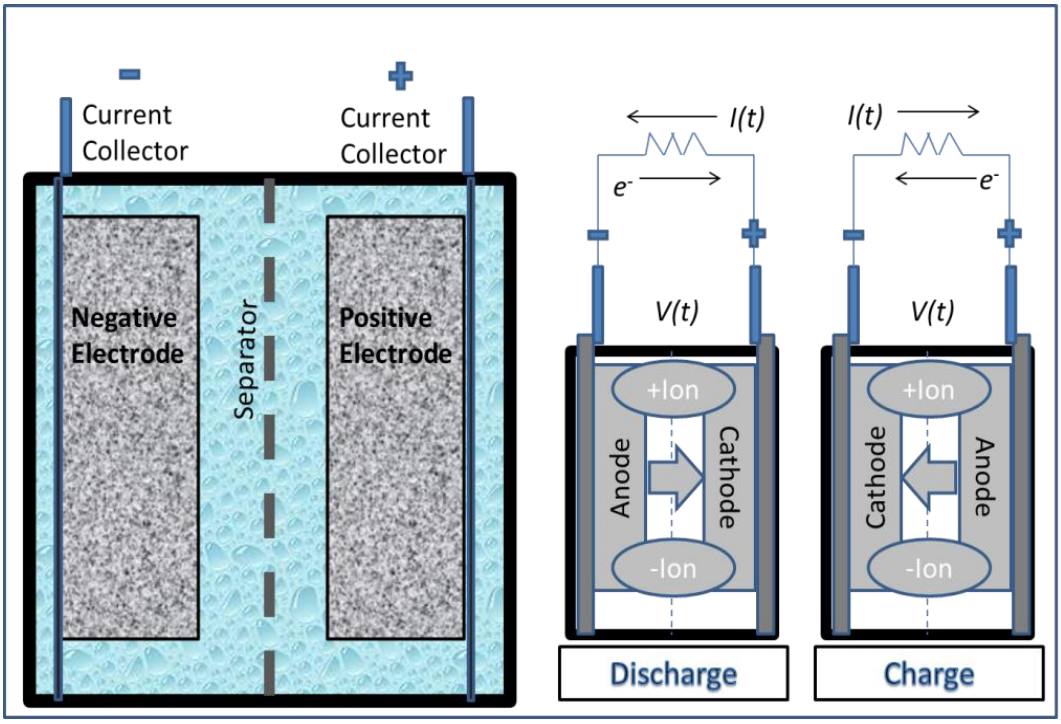

Figure 2 Schematic of the working principle of a typical electrochemical cell.

An electrochemical cell converts chemical energy into electrical energy or reversibly, converts an applied electrical energy to facilitate chemical reactions. A basic battery cell consists of four primary components – a positive and negative electrode, a separator, and an electrolyte along with current collectors attached to each end of the electrode. An electrode is made up of a material that is an electronic conductor i.e. it allows the passage of electrons through it. Depending on the application and chemistry, the materials selected as the positive and negative electrodes will differ. In order to aid the selection process, galvanic series chart can be useful. A Galvanic series is an experimentally compiled list of common materials and their relative activity or potential when compared to a standard hydrogen electrode. Generally, the further apart two electrode materials sit in a Galvanic series, the higher is their potential difference. Thus, materials with a larger potential difference used in a cell are able produce a desirable high voltage. Table 2 is a snippet of a galvanic series chart with a few elements' potentials listed in reference to hydrogen.

Table 2 Electrochemical series of metals and their standard potentials.

Metals	Standard Potentials
Au/Au^{3+}	+1.50
Hg/Hg^{2+}	+0.86
Ag/Ag^{+}	+0.8
Cu/Cu^{2+}	+0.34
$H_2/2H^{+}$	0.00
Pb/Pb^{2+}	-0.12
Ni/Ni^{2+}	-0.24
Cd/Cd^{2+}	-0.40
Fe/Fe^{2+}	-0.44
Zn/Zn^{2+}	-0.76
Al/Al^{3+}	-1.66
Mg/Mg^{2+}	-2.35
Na/Na^{+}	-2.71
K/K^{+}	-2.92
Li/Li^{+}	-3.02

Apart from the electrodes, the selection of the appropriate separator and electrolyte material is equally important. As the name suggests, separators are the component that separate or keep a distance between the two electrodes. Separators serve two primary functions: while having to keep the positive electrode physically apart from the negative in order to prevent any electronic current passing between them, they also have to permit an ionic current with the least possible hindrance [6]. Upon examination, it is apparent that these requirements contradict each other. Hence, the best possible type of material to meet both these needs is a porous type separator. This porous material should be capable of allowing the passage of ions and at the same be a barrier against the passage of electrons. Therefore, separators should be electronically insulating but

ionically conducting materials. Separators themselves do not participate in the electrochemical reaction. They are inert and should remain so over a wide temperature range. Some common separator materials are polypropylene (PP) and polyethylene (PE). A prominent separator is manufactured by the company Celgard. The Celgard material is made up of a tri-layer setup- PP/PE/PP which offers good shutdown and thermal stabilities.

Electrolytes are another component of the battery that serves very important functions. The term '*electrolyte'* refers to an ion-conducting solution which consists of a solvent S and a salt. An ideal electrolyte must possess several attributes in order to be useful for a practical battery. Some of these characteristics are low toxicity, high conductivity, stability over a large electrochemical window, stability over a large temperature range, low price etc. [7]. Some common electrolytes are dimethyl carbonate (DMC), ethyl methyl carbonate (EMC), sulfuric acid, potassium hydroxide, gel or polymer electrolytes etc. The choice of separator material depends heavily on the type of battery and its intended application.

Discharge Operation - During the discharging process, the chemical energy of the cell is converted into electrical energy or the current which powers the device or load in question. When the cell is discharged, the electrons flow from the anode to the cathode through the external load. In this case, the anode is the electrode being oxidized since it loses electrons. Consequently, the cathode is the electrode that is being reduced due to the acceptance of electrons. The anions and cations flow to the anode and cathode respectively, thereby completing the circuit.

Charge Operation - During the charging of the cell, the process described above is basically reversed. The cell is now provided with electrical energy which is used to generate chemical energy in the cell. The anode now becomes the positive electrode because that's the electrode where oxidation takes place. The cathode is the negative electrode which is reduced in the process.

With the recognition of the important functions and characteristics required of the various components and the cell as a whole, several modern cell chemistries have been developed over the years. Batteries are characterized by the function they need to serve depending on the power and energies available from them in order to power a load. The theoretical voltage of these batteries is also higher as compared to the other two cell chemistries. Another important parameter is the energy efficiency of a battery. The coulometric efficiency of Li-ion cells is also the largest followed closely by lead acid batteries with Ni-MH being the least efficient. One of the major drawbacks of the earlier batteries was the problem of 'memory effect'. This was a phenomena observed in batteries where the cell would 'remember' the level of discharge that was drawn previously and would only discharge to the same level in the next charge cycle. With the invention of Li-ion batteries, this problem has been completely eliminated.

Table 3 gives a comparison between several properties of Li-ion, Nickel-Metal Hydride (Ni-MH) and Lead Acid (Pb-Acid) batteries which are some of the most common secondary batteries today. Lead acid batteries were one of the older cell chemistries. These batteries are primarily used in ignition applications. As can be noted from the table, Li-ion batteries have the highest power and energy densities. This is precisely the reason that these batteries have gained tremendous traction in the past few years. The theoretical voltage of these batteries is also higher as compared to the other two cell chemistries. Another important parameter is the energy efficiency of a battery. The coulometric efficiency of Li-ion cells is also the largest followed closely by lead acid batteries with Ni-MH being the least efficient. One of the major drawbacks of the earlier batteries was the problem of 'memory effect'. This was a phenomena observed in batteries where the cell would 'remember' the level of discharge that was drawn previously and would only discharge to the same level in the next charge cycle. With the invention of Li-ion batteries, this problem has been completely eliminated.

Table 3 Comparison of Pb-acid, Ni-Mh, and Li-ion performance. Inspired and redrawn based on [3].

	Lead Acid	Nickel-Metal Hydride	Lithium-ion
Theoretical			
Voltage	1.93	1.35	4.10
Specific Energy (Wh/kg)	166	240	410
Practical			
Specific Energy (Wh/kg)	35	75	150
Energy Density (Wh/L)	70	240	400
Coulometric Efficiency	0.80	$0.65 - 0.70$	> 0.85
Energy Efficiency	$0.65 - 0.70$	$0.55 - 0.65$	~ 0.80
Specific Power, 80% DOD (W/kg)	220	150	350
Power Density(W/L)	450	> 300	> 800

Lithium-Ion

As described in the general construction of an electrochemical cell, Li-ion cells are also assembled with the four major components – negative and positive electrodes, electrolyte and a separator. Typically, the positive electrode is made up of a lithium metal oxide. Some common cathode chemistries include Lithium Cobalt Oxide ($LiCoO_2$), Lithium Iron Phosphate ($LiFePO_4$) and Lithium Manganese Oxide ($LiMn_2O_4$). The metal in the cathode is the transition metal. The anode is typically made up of some carbon or carbon derived material. Some common anode materials are graphite and

carbon fiber composites. These electrodes are attached to metallic current collectors. In current collectors of lithium-ion batteries, aluminum and copper are typically used as substrates at the cathode and anode respectively. Electrode active materials are coated on current collectors followed by drying to create electrodes. Despite being comprised of a very thin foil, current collectors show sufficient mechanical strength. The anode current collectors consist of materials such as copper or nickel which are electrochemically inactive or stable within the working potential of carbon electrodes. In particular, copper is relatively stable toward reduction while nickel drives up the cost of the cell. For cathode, it is important to avoid oxidation of metal current collectors at high potential. Copper cannot be used for cathodes as oxidation occurs at 3 V. Considering various factors of cost and electrochemical stability in the operating range, aluminum is the most appropriate current collector for the cathode. The lithium ions insert into or deinsert from the active materials via an intercalation process. This intercalation of Lithium ions comprises of two motion mechanisms- diffusion and migration.

In the positive electrode during charge, the active material is oxidized and lithium ions are deintercalated as follows:

$$Li_{1-x}CoO_2 + xLi^+ + xe^- \underset{\text{charge}}{\overset{\text{discharge}}{\rightleftharpoons}} LiCoO_2 \qquad \textit{Eq. (1)}$$

In the negative electrode during charge, the active material is reduced and lithium ions that migrate from the positive electrode and through the electrolyte and separator are intercalated in the reaction.

$$Li_xC \underset{charge}{\overset{discharge}{\rightleftharpoons}} C + xLi^+ + xe^- \qquad \text{Eq. (2)}$$

Reactions 1 and 2 reverse for discharge. These reactions produce a theoretical cell voltage of 4.1 V, much higher than either the Ni–MH or Pb–acid cells. The reactions shown above are for a representative cell chemistry of lithium cobalt oxide. There are several advantages to Lithium-ion batteries as compared to other technologies. Firstly, they have a low self-discharge rate (in contrast to Ni-MH batteries). Secondly, as can be seen from the table, they have the highest power and energy densities among the others which is the major factor in the choice for the utilization of these batteries for vehicle electrification. Lithium- ion batteries are pervasive in several applications across various industries like portable electronics, medical devices, automobiles etc. With the merits of high energy density, long cycle life, little to no memory effect and high specific capacity, it is no wonder that these batteries are ubiquitous in their market spread as a powerful energy storage device [8].

However, as Li-ion technology stands today, it is evident that in order to achieve complete vehicle electrification, there is a significant gap in performance that needs to be bridged when compared to a traditional IC engine vehicle. The materials roadmap is a comprehensive schematic of current position of Li-ion technology today. Most of the well-known chemistries such as LCO, LFP and LMO offer a maximum of up to 300 mAh/g of theoretical capacity. The materials roadmap depicts a few materials that have recently captured the interest of many researchers. For example, with a theoretical capacity of 1675 mAh/g, elemental sulfur has been considered as one of the most

promising alternative cathode materials for high-capacity energy storage [9]. Another promising alternative is Li-Air batteries. Tesla's Model S car, while a breakthrough in vehicle electrification, does so at an astronomical price point that is not feasible for the everyday man's pocket. Air being a no-cost material, has gained tremendous interest for its abundance and economic feasibility. However, with any new technology, the initial excitement is sure to dwindle down as more explorations unearth unresolved challenges with the new battery technologies. And so, while half of the battery community is dedicated to solving those newer challenges, the other half is immersed in attempting to perfect the existing battery technologies. Simple electronics only require charging at periodic intervals and most of that charging is done at a pre-specified low charging rate. Electric vehicles on the other hand are an entirely different arena. EVs and HEVs require high power and current densities for the braking and accelerating functions typical of a vehicle. This rapid charge–discharge cycling of the battery pack requires sophisticated battery management systems to regulate the current in and out of the pack in real time. An effective battery management system sets the current limits low enough to maximize the battery life and ensure safety but high enough to maximize power output [3]. While dangerous situations concerning Li-ion batteries are few and far between, there certainly have been several reported incidents regarding their safety. Of the most recent incidents, there was one where the phone company Samsung recalled their Samsung Galaxy S7 model due to several reports of phones catching fire and exploding in people's homes. Another report from 2013 showed that the auxiliary power unit in a Japan Airlines Boeing 787 had shut down due to the lithium-ion batteries catching fire. While no

passenger was on the plane during the occurrence of the incident, this could have had serious ramifications for any of the passengers or the crew. Incidents like these reinforce the need for enhanced safety of Lithium-ion batteries.

Objective of this Study

The objective of this study is to gain insight about the behavior of Lithium-ion cells under overcharge abuse conditions. In order to resolve the safety issues of these cells, the thermal aspects must be understood. As previously stated, current safety measures may be acceptable for small capacity batteries. However, if these cells are to be successfully scaled up and implemented for use in EVs and HEVs, safety of the Li-ion cells must be drastically improved.

CHAPTER II

LITERATURE REVIEW

Degradation in Li-Ion Batteries

Despite their superior performance as compared to other cell chemistries, Li-ion batteries contain materials that are reactive, volatile and flammable under certain conditions which may be construed as a threat to safety [10].With the increasing interest in the utilization of these batteries for vehicular applications, their safety and abuse tolerance response needs to be explored. Thermal runaway is one of the issues of paramount importance that still needs to be resolved in the realm of Li-ion battery research. Specifically, these batteries that are used in applications like aviation, ground and water transportation need to be held to rigorous safety standards as compared to ones used in portable electronics applications. Lithium-ion batteries have a limited window of stability in terms of voltage and temperature [11]. When these batteries are operated outside of the manufacturer recommended windows, certain reactions occur in the cell which lead to the accelerated heat release previously quoted as thermal runaway. As the temperature (or voltage) of the cell increases beyond the safe limit, the thermal runaway can cause catastrophic damage and even lead to the cell ignition.

There have been several attempts made by researchers to study the thermal behavior of lithium-ion batteries. Some of these works have been purely experimental, some purely model-based and some are a combination of both. There are several degradation reactions occurring in Li-ion batteries that can contribute to thermal runaway. . Over the years, there has been somewhat of a consensus as to the events that

happen within the cell that lead to thermal runaway. Spotnitz and Franklin [12] wrote a comprehensive survey of the thermal behavior of the cell components in Li-ion batteries.

The metastable layer known as the Solid Electrolyte Interphase begins to decompose upwards of 90 °C. The SEI, also known as the anode/electrolyte interphase is a metastable layer that forms on the negative electrode. This layer usually forms within the first two charge cycles. During first charge of the Li-ion battery the electrolyte undergoes reduction at the negatively polarized graphite surface. This forms a passive layer comprising of inorganic and organic electrolyte decomposition products [13]. This decomposition opens the door to a whole host of deteriorative reactions. The SEI acts as a protective layer for the anode surface. Ideally, this layer protects the negative electrode from coming into direct contact and participating in a direct reaction with the electrolyte. Not only does this prevent the decomposition of the electrolyte, but since the SEI is an electronically insulating layer, it only allows ions to pass through while preventing the passage of electrons through it. This layer is only metastable; which means that, at higher temperatures and under abusive conditions, this layer may decompose exothermically at around 90-120°C [12]. Without this electronically insulating layer, the intercalated lithium can react with the electrolyte in an exothermic reaction which ultimately contributes more heat triggering the progression of thermal runaway. As temperature rises above 120 °C, decomposition of the solid electrolyte interface (SEI) layer follows, leading to reduction of the electrolyte at the lithiated graphite negative electrode [14]. The temperature rise due to SEI decomposition has been reported to be very small up to

2 °C. However, the subsequent negative electrode/solvent reaction has been shown to raise the temperature of the cell by approximately 100 °C.

$$(CH_2OCO_2Li)_2 \rightarrow Li_2CO_3 + C_2H_4 + CO_2 + \frac{1}{2}O_2 \qquad \textit{Eq. (3)}$$

or

$$2Li + (CH_2OCO_2Li)_2 \rightarrow 2Li_2CO_3 + C_2H_4 \qquad \textit{Eq. (4)}$$

The depletion of the SEI layer is heavily dependent on the composition of the electrolyte. Following the decomposition of the SEI layer, the intercalated or metallic (deposited) lithium can react with the electrolyte since it is not protected by the SEI layer anymore.

Several researchers have done ARC and DSC studies. Through these studies, the various temperature peaks and values for enthalpy, activation energy, heat of reaction and frequency factor have been reported [15-17].

In commercial lithium ion batteries, a very popular binder used is polyvinylidene fluoride (PVDF). PVDF is commonly used for both the positive and negative electrodes due to its good electrochemical stability and high adhesion to electrode and current collector materials [18]. Metallic or intercalated lithium can possibly react with a fluorinated binder. Again, various studies have reported values for the heats of

reaction, enthalpies and reaction temperatures of between 200-350 °C depending on the cell chemistries [17, 19, 20].

Traditional aqueous electrolytes are not suitable for use in lithium-ion batteries due to their narrow range of electrochemical stability. Since the aim with any battery chemistry is to achieve a high voltage, electrolytes tailored to the application are necessary. As previously mentioned, DMC and EC are some of the commonly used electrolytes in Li-ion batteries. The last reaction in the 'moderate temperature rise zone' can be due to the electrolyte decomposition. Electrolyte decomposition is an ambiguous topic and it is very difficult to find commonality between the various studies. The cell reactions are heavily dependent on the type of electrolyte used. And even though materials like DMC and EMC are common, their percentages, the presence or lack of additives and several other factors greatly affect the results achieved in the experiments. In the work by Roth, the role of electrolyte solvent decomposition on thermal abuse response was investigated for two compositions: ethylene carbonate: ethyl methyl carbonate (EC:EMC) (3:7) \1.2M LiPF6 and ethylene carbonate: propylene carbonate: dimethyl carbonate (EC:PC:DMC)(1:1:3)\1.2M LiPF6. Electrolyte additives were also examined to determine the effect on low-temperature stability, flammability and overcharge protection. In ARC profiles of two different solvent compositions, it was shown that the EC:PC:DMC solvent showed the lowest reaction rate. This study was further extended to explore the solvent effects for different cell chemistries of $LiNi_{0.85}Co_{0.1}5O_{2,}$ $LiNi_{0.80}Co_{0.15}Al_{0.05}O_2$and $LiCoO_2$. The cells with PC containing electrolyte showed reduced heating rates for all three cathode chemistries.

Electrolyte additives have also been shown to improve the overcharge tolerance of Li-ion batteries. The work by Feng et al [21] incorporates the use of methylbenzenes as possible electrolyte additives for improving the overcharge performance. Based on the voltammetric behaviour of a series of methyl-substituted benzenes in 1 M LiPF6/EC-DMC electrolyte, xylene was selected and tested as an electrolyte additive for overcharge protection of Li-ion batteries. From the overcharge curves, CV behaviour and SEM observations of the cells in the presence of xylene, it was found that the additive can polymerize at the overcharged voltage to form a dense layer of isolating polymer film at the cathode surface, which blocks off further oxidation of the electroactive material and electrolyte and, therefore, improves the overcharge tolerance of the Li-ion battery. In addition, the xylene additive was shown to only slightly influence the cycling behavior of the cells. In sum, the thermal behavior of Li-ion cells and the electrolyte decomposition reactions are extremely sensitive to the composition of the electrolyte.

Moving from the moderate to the most debilitating reactions, the next important phenomenon is the reaction of the cathode positive material. The heat released from the anodic reactions triggers the decomposition of the positive active material. The decomposition of the cathode and subsequent oxidation reaction with the electrolyte/solvent is considered to be the most exothermically abusive reaction which can lead to a temperature rise of greater than 100°C. The solvent oxidation and the cathode decomposition are considered as a coupled reaction because the oxygen release from the cathode oxidizes the solvent. Abuse tests done on prismatic Li-ion cells in the

work by Leising et al. [22] identifies and confirms the cathode to be the source of major heat production in the cell. A similar conclusion was derived from the work by Zhang et al. The study indicated significant exothermic reaction between some commonly cathode materials such as Li_xNiO_2, Li_xCoO_2 and $Li_xMn_2O_4$and electrolytes. The reactions were postulated to be due to contributions from the solvents and the salt in the electrolyte. Depending on the stoichiometry, the material and the degree of delithiation, the onset temperatures were reported to be between 200-230 °C [23].

Abuse Tests

Deliberate abuse testing of cells is an indispensable method in order to gain valuable insight into the safety behavior and thermal runaway tolerance of Li-on cells. There are several abuse testing methods in Lithium-ion batteries that can provide valuable information about thermal runaway such as overcharge, overdischarge, internal and external short circuit, physical deformation, penetration etc. [12, 24, 25]. These tests simulate the potential hazards that a cell can be exposed to during service. These tests can be characterized into three main types: thermal, mechanical and electrochemical abuse tests. Each of these types will be reviewed briefly.

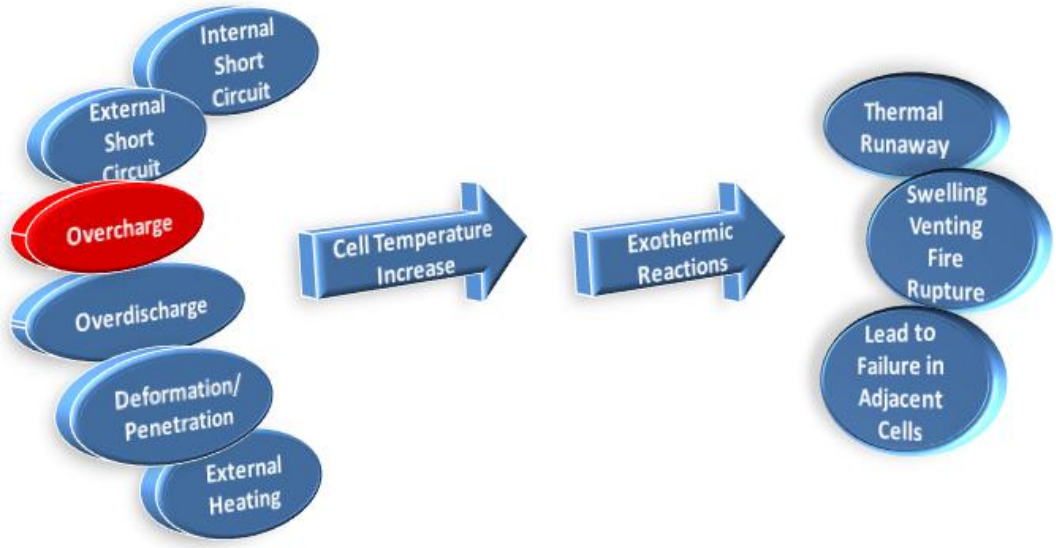

Figure 3 Schematic of the various degradation mechanisms possible in Li-ion cells and their consequences leading up to a catastrophic event. Inspired and redrawn based on [10].

Thermal Abuse Tests

1. Heating Test: External heating or oven tests are a common abuse testing method. These tests include heating the cells to excessive temperatures, typically 150°C for consumer batteries. In the guidelines for the heating test of secondary lithium cells, the heating condition is reported to be 130 °C for 1h. Typically when cells are abuse tested, this is done so on fresh cells. Even though it is important to test fresh cells and characterize the materials' thermal tolerance, it might be even more prudent to abuse test cycled cells because they behave differently than fresh cells. In a heating test done by Tobishima and Yamaki [26], the heating temperature was varied in 5 °C increments and these constant temperatures were held until the cell temperature started to decrease. The highest temperature at which the cell did not smoke was determined as the thermal stability limit of the cell. Commercial cylindrical lithium ion cells with a 1.27 Ah capacity were used for the tests. The heating tests were done at 150 °C and 155 °C respectively. When the cells were charged under normal charging conditions, it was found that the cells did not smoke at 150 °C but smoked at 155 °C. Hence, 150 °C was determined to be the thermal stability limit of these cells. A more careful investigation is necessary when the thermal stability of the cells is reduced due to cycling [27]. In another test done by Larsson et al [10], cylindrical 18650 cells were also subjected to an external heating (also known as thermal ramp or oven) test. The thermal runaway temperature was observed to be at 220 °C while the maximum temperature that the cell reached was 743 °C at the surface (the

internal temperature must have been even higher). Based on published values for different cell types and the temperature increase of 523 °C, the energy release was estimated to be 15.6 kJ (4.33 Wh). A derivative of the average cell temperature also showed that the thermal runaway temperature was 220 °C and the rate of temperature increase was 5000 °C/min.

2. Fire Tests: Fire tests are another valuable thermal abuse test that can provide a plethora of useful information. For example, the work done by Larsson et al [28] incorporates fire tests. Electrolytes usually contain flammable organic solvents. Depending on the solvents used, some of them are volatile even a relatively low temperatures of 100 °C or less. A common salt lithium hexafluorophosphate has a limited window of thermal stability. $LiPF_6$can react with even the slightest traces of moisture to form toxic gases such as lithium fluoride (LiF) and hydrogen fluoride (HF). The reactivity and stability of these gases has been studied under normal temperatures, but not under high temperatures simulating the event of a fire or explosion. Six cells containing LFP cathodes were abuse tested. The cells were exposed to a controlled propane fire in order to evaluate the rate of heat release (HRR), emission of toxic gases as well as cell temperature and voltage under this type of abuse. The results showed that high state of charge (SOC) values gave high HRR peaks and the temperature and voltage measurements confirmed that the EiG battery cells with high SOC value gave a more reactive response. A rapid temperature increase and early voltage breakdown was observed. Thus, the HRR peaks observed were in a range from

13-57 kW for batteries of 100 Wh energy capacity. The amount of HF gas released was found to be between 5 and 124 mg Wh^{-1}. Extrapolation of data shows that 400-1200 g of HF could be released from a 10kWh PHEV battery. If this amount were to be released in a passenger compartment of 5 m^3, the equivalent concentration of HF would be between 80-240 gm^{-3}. This magnitude is higher than the acceptable short time exposure levels.

Mechanical Abuse Tests

Mechanical abuse tests help to identify and simulate the conditions in the event of a vehicular crash and how the mechanical deformation impacts battery integrity. Some common mechanical abuse tests include nail penetration and impact (deformation).

1. Deformation Tests: In a typical crush test, some sort bar is used to deform the battery which initiates a short circuit in the cell. In the work done by Sahraei et al [29], 18650 lithium-ion cells were tested under indentation by a hemispherical punch, lateral indentation by a cylindrical rod, compression between two flat plates and three point bending. The results from the test included force, displacement, voltage and temperature versus time. A finite element model of the cells was also developed. Their model was able to predict the response of a single cell for different abuse cases. The model was also able to predict the onset of short circuiting of the cell which is a necessary (but not sufficient) condition for the initiation of thermal runaway. In another work by Lam et al., mechanical abuse experiments were performed on commercially obtained 18650 Li-ion batteries and pouch cells [30]. Blunt rod indentation was performed in both the

axial (parallel to the cylindrical axis) and transverse (normal to the cylindrical axis) directions of cylindrical cells as well as horizontally (through the flat face of the cell) and vertically (through the side of the cell) through prismatic pouch cells. Through CT imaging, it was shown that extensive damage to the cell components was necessary in order to cause a failure to the cell. For the short to occur, significant penetration into the electrodes was necessary. Overall, a significant effect of cell construction on the results obtained from mechanical tests was cited as a conclusion to the work.

2. Nail Penetration: Nail penetration is another common method in order to generate a short circuit event in the cell. This type of test is useful in simulating the event of an internal short circuit in the cell. Generally, it is very difficult to avoid internal shorting of the cell. This is why metallic lithium deposition and dendrite formation are an ongoing concern in Li-ion batteries due to the subsequent internal shorting that occurs in the cell. Nail penetration tests are no longer described in the UL 1642 standard [31]. These tests are still widely used for exploring the short circuit issues in Li-ion cells.

Electrochemical Abuse Tests

The third category of abuse testing can be categorized as the electrochemical type. Within this category, the types of tests can even be divided into sub-categories of direct and indirect electrochemical tests.

Indirect Electrochemical Tests

1. Internal Short Circuit: These are coined as ‘indirect’ tests because they may occur accidentally or as a consequence of another reaction happening in the cell. Internal short circuit tests can be classified into this type. In fact, nail penetration tests causing internal short circuiting of the cell have already been discussed in a previous section.

Direct Electrochemical Tests

1. External Short Circuit: In an external short circuit test, usually a low resistance (<5 mΩ) is connected across the terminals of the battery. The battery may be preheated. In this test, current flows through the battery generating heat. The battery is heated internally due to current flow, but the external circuit can dissipate heat also [12].Two EiG lithium-ion cells of different designs (old and new) were tested in an external short circuit test done by Larsson and Mellander [10]. It was found that the results did not vary among the two different designs of the cell. Events such as swelling and burning of the cell tabs were noticed in the test, but the cell was not found to reach thermal runaway. The peak current reached by the cell was almost 900 A. Since a short circuit test does not add any

energy to the system, these tests are considered to be a more mellow form of abuse testing.

2. Overdischarge: As the name might suggest, overdischarge is a phenomenon that occurs when a cell is discharged beyond a certain limit. The lower limit in this case is determined by the cell manufacturer based on the chemistry of the cell. For example, the cells that are key to this study are Panasonic NCR18650B li-ion cells. For normal operation, the voltage window given by Panasonic in its datasheet is 2.5 to 4.2 V [see Table 4]. Consider three lithium-ion cells at arbitrary states of charge, two fully charged and one 50% discharged. If these are connected in series and then connected to a device like a flashlight, the partially discharged cell will fully discharge before the other two, and will be forced into polarity reversal by the other cells if the flashlight is left on. Although this does not necessarily cause a safety hazard, it forces electrodes outside their normal potential ranges and adversely affects the cycle life [32]. Several works have been done where redox shuttles have been reviewed, tested and employed in order to improve the overdischarge (and overcharge) performance of the cells [21, 23, 33].
3. Overcharge: In this test, a cell is allowed to charge beyond its recommended 100% state of charge (SOC) up to a predetermined maximum voltage limit (typically 10 or 12 V). As the name suggests, overcharge is a condition in which a cell's potential rises above the upper limit as recommended by the manufacturer for safe operation of the cell as shown in Table 4. Prevention of

overcharge is critical to achieving long lifetimes and averting catastrophic failure events in lithium-ion batteries [34]. This report focuses on the understanding of the overcharge phenomenon of Li-ion batteries

What is Overcharge?

Table 4 Panasonic NCR18650B Lithium ion manufacturer provided specifications.

Specifications	Listed
Rated Capacity(1)	Min. 3200mAh
Capacity(2)	Min. 3250mAh Typ. 3350mAh
Nominal voltage	3.6V
Charging	CC-CV, Std. 1625mA, 4.20V, 4.0 hrs
Weight (max.)	48.5 g
Temperature	Charge*: 0 to +45°C Discharge: -20 to +60°C Storage: -20 to +50°C
Energy Density(3)	Volumetric: 676 Wh/l Gravimetric: 243 Wh/kg

(1) At 20°C (2) At 25°C (3) Energy density based on bare cell dimensions.

Although overcharge for a single cell may not be a significant problem, when the entire battery pack gets damaged due to thermal runaway even in a single cell, the results can be drastic. As previously mentioned, every commercial battery comes with a certain set of specifications as recommended by the manufacturer for safe operation of the battery. In the case of Panasonic Li-ion NCR18650B [35] cells used in the study, the

voltage window of safe operation is prescribed to be from 2.5 V to 4.2 V. With that description in mind, overcharge of the cells is thus said to occur when the cell is charged beyond the upper limit of 4.2 V.

Cell Protections

Commercial Lithium-ion cells have several protective measures built into them to protect them from abusive conditions. As discussed, some of these conditions can lead to a current and temperature surge in the cells leading to potentially hazardous consequences. Hence the need for in-built cell protections has been realized. Some of these measures are shutdown separators, positive temperature coefficient resistors (PTC), current interruption device (CID), pressure sensitive rupture disks, vents etc. The most basic safety device in a battery is a fuse that opens on high current. Some fuses open permanently and render the battery useless; others are more forgiving and reset. In order to find better solutions, manufacturers have included various other safety measures within the cell as discussed below [36].

Shutdown Separators

Shutdown type separators have also been implemented in commercial batteries as one of the primary ways for abuse protection. A shutdown separator inhibits ion-flow by melting process when exceeding a certain temperature threshold. However, there can be some drawbacks associated with it. Firstly, separator shutdown is an irreversible phenomenon. Secondly, even if a separator meltdown occurs, there is some current that is able to pass through micro pores in the separator which are formed due to high temperatures. Thus, this can pose a safety hazard if the battery is not disposed of immediately after separator malfunction. Early versions of Li-ion cylindrical cells primarily used polypropylene single layer separators. However, most of the prismatic Li-ion cells manufactured today either contain a PE single layer or a PP/PE/PP tri-layer separator. Since polyethylene has a lower melting temperature than polypropylene-, polyethylene-based separators offer lower shutdown temperatures [36]. There have been several studies in which various separator materials have been tested in regards to the improvement in overall thermal stability of cells. In the work done by Roth et al., separator response as a function of temperature and high voltage was measured for Li-ion 18650 cells. The separators used for their study were the Celgard Trilayer shutdown separator and SEPARION non-shutdown separator. The Celgard material is a shutdown separator consisting of three layers of polypropylene (PP) and polyethylene (PE) in a PP/PE/PP configuration while the Degussa SEPARION® material is a single layer of polyethylene terephthalate (PET) impregnated with alumina/silica [37]. Shutdown

separators were found to delay the thermal runaway, yet it is important to realize that these separators only offer a delay – not complete protection from thermal runaway.

Positive Temperature Coefficient (PTC)

The resistance of a PTC device increases with an increase in temperature. The active component in a PTC is a highly filled composite of conductive filler and polymer binder. When the temperature increases, the binder starts to expand thereby leading to an increase in the resistance of the composite. PTC is ideally supposed to be reversible. PTC devices are current limiting devices. PTC is especially useful for damage caused due to external shorting. It protects against current surges. The current limiting capability and activation temperature can be modified by tailoring the active material used.

- Built-in to almost all 18650's
- Inhibits high current surges
- Protects against high-pressure, over temperature
- Resets and does not permanently disable the battery when triggered.
- May not work when module included multi-cell series and/or parallel configurations [38].

Figure 4 A positive temperature coefficient device retrieved after disassembly from an ovecharged 18650 Li-ion cell. The two plates sandwich a blackish phase change material which transforms into an amorphous material upon activation.

Figure 4 is a picture of the PTC device taken after disassembly of a Panasonic 18650 Li-ion cell. The two metallic disks are separated by a thin layer of conductive polymer. Conductive-polymers are phase change materials. At elevated temperatures, these materials change into an amorphous structure. The expansion from this phase change inhibits current flow and increases the resistance of the cell thereby effectively bringing the current down to an acceptable level [39].

Current Interrupting Device (CID)

A CID can be indirectly activated by high temperature. Increase in the temperature inside the cell causes an increase in the vapor pressure of the non-aqueous electrolyte solvent, which triggers a break in the contact between the jelly-roll and header assembly.

CID is widely used in cylindrical Li-ion assemblies. CIDs are built-in to almost all 18650s.

- They are not visible without opening the battery
- Incorporated together with the PTC
- May not work when module includes multi-cells series and/or parallel configurations [38].

Because overcharge leads to thermal runaway in lithium-ion cells, many cell designs include built-in mechanisms to prevent overcharge. Overcharge can lead to significant gas generation within a cell prior to the cell entering a thermal runaway condition. In prismatic form factors, and particularly in cells with thin cases or with soft-pouch cells, gas generation within the cell will result in cell swelling and may force electrodes apart, effectively curtailing the transfer of ions and interrupting charging. This process can prevent thermal runaway of the cells, but is not always effective. The geometry of cylindrical cells prevents separation of electrodes if gas generation occurs. Cell designers have developed mechanical charge interrupt devices (CIDs) for cylindrical cells used in consumer electronic devices. On activation, CIDs physically and irreversibly disconnect the cell from the circuit. Although CIDs are usually described as overcharge protection devices, they will activate if anything causes cell internal pressure to exceed the activation limit. This could include overcharge, cell overheating, significant lithium plating followed by electrolyte breakdown, mild internal shorting, and/or significant cell over-discharge. Proper design and installation is required for

reliable operation of CIDs. CIDs must also be appropriately matched to cell chemistry so that overcharge conditions result in sufficient gas generation prior to thermal runaway to activate the CID. If a CID is not properly matched to cell chemistry, low current overcharge or very high over currents may not activate a CID sufficiently early to prevent cell thermal runaway.

Figure 5 shows two disassembled CIDs. On the left is a CID that hasn't been employed. On the right, a visible gap can be seen between the outer ring and the smaller ring in the center. This indicates that the CID was activated in this cell which broke physical contact between the jelly roll and the header, thus protecting the cell.

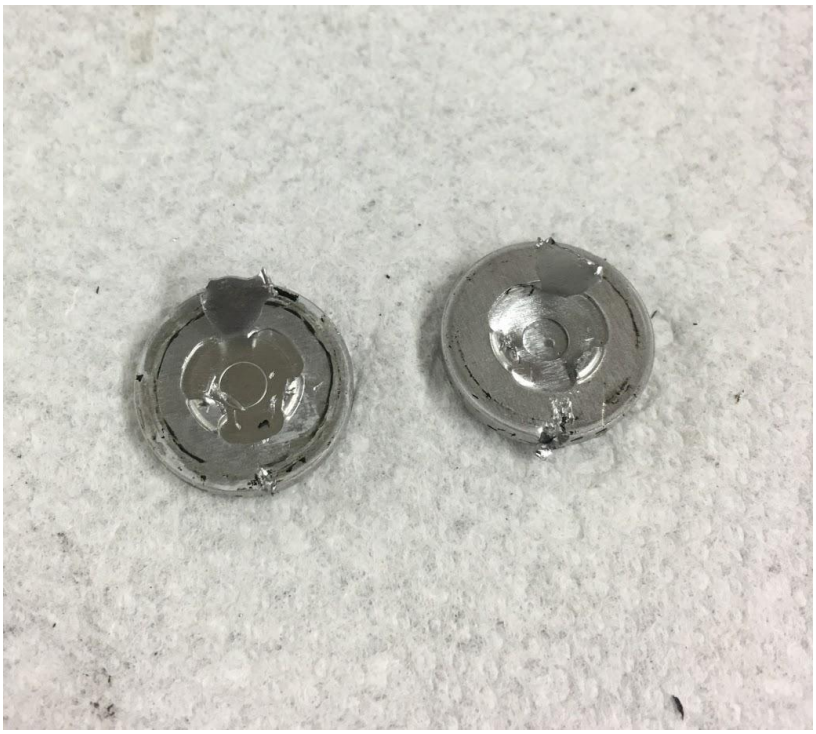

Figure 5 Two current interrupt devices obtained from an overcharged 18650 Li-ion cell.

Safety Vents

With many cell chemistries, the electrochemical process can give rise to the generation of gases, particularly during conditions of over charge. This is called gassing. If the gases are allowed to escape, the active mass of chemicals in the cell will be diminished, permanently reducing its capacity and its cycle life. Furthermore the release of chemicals into the atmosphere could be dangerous. Manufacturers have therefore developed sealed cells to prevent this happening. Sealing the cells however gives rise to a different problem. If gassing does occur, pressure within the cell will build up, this will usually be accompanied by a rise in temperature which will make matters worse, until the cell ruptures or explodes. To overcome this second problem sealed cells normally incorporate some form of vent to release the pressure in a controlled way if it becomes excessive. This is the last line of defense for an abused cell if all the other protection measures fail. Cells are not meant to vent under normal operating conditions. Usually during abuse, other devices described such as the PTC and CID override the vent.

While these measures may be sufficient in some applications, the scaling up of Lithium-ion batteries for use in automotive requires a more stringent approach to safety and protective measures. There are several complex processes that occur during the overcharge of Lithium-ion batteries. These may include but are not limited to: 1) An increase in cell temperature 2) Decomposition of the electrolyte 3) Lithium plating 4) Decomposition of electrodes 5) Gas evolution 6) Melting of separator etc. In order to address these issues, one or more of these approaches can be implemented:

1. Increasing the exposed surface area of the cell will allow proper dissipation of the heat energy to the ambient
2. Minimizing or eliminating the side reactions occurring during overcharge [40].

However, almost all the applications today require the batteries to be compact in size which eliminates solution 1. Thus, as it stands now, most research in Lithium-ion battery safety is geared toward finding a solution for the prevention of unwanted side reactions.

According to literature, there are several avenues towards which overcharge research is geared. Some of these may be aimed at characterizing better and thermally more stable electrode materials. For example, in the work done by (improvement of overcharge perform) it was found that when two cells with an LFP cathode but with differing anode materials were tested, significantly varied results were observed. The two anode materials compared were $Li_4Ti_5O_{12}$and graphite. It was found that the cell with the $Li_4Ti_5O_{12}$ showed better thermal runaway performance than its graphite counterpart [41]. Similarly, another study done compared different cathode materials and their behavior during overcharge. Two types of commercial 18650 Li-ion cells with different cathode materials were used in this work. The first type used $LiCoO_2$ as cathode active material (LCO-Graphite cell) and the second type used $LiMn_2O_4$ (LMO) as cathode active material (LMO-Graphite cell).The LCO-Graphite cells exhibited a thermal runaway behavior from 50% to 120% SOC, while LMO/Graphite cells exhibited a thermal runaway behavior from 75% to 120% SOC. In the case of 120% SOC, overcharge, both cells presented a thermal runaway behavior, but there was a significant

difference between the onset temperatures of thermal runaway. The onset temperatures of thermal runaway behavior at 120% SOC of the LCO Graphite and LMO-Graphite cells were 176.4 °C and 189.8 °C, respectively. The cell using $LiCoO_2$ as cathode material was found to be more thermally unstable than the cell using $LiMn_2O_4$ [42]. In the work done by Larsson and Mellander, lithium-ion cells which were LFP based showed better thermal stability than their cobalt based counterparts [9]. Thus, it is widely published in literature that cobalt based cathodes are inherently more unstable than other chemistries. Some other works are geared toward finding ways to use electrolyte additives to improve cell performance and these have already been discussed in a previous section.

Other works aim to trace the step by step process of overcharge and perhaps the charging rate dependence of Lithium-ion cells [43, 44]. The research by Finegan et al [41] aims to probe the degradation mechanisms leading up to the overcharge-induced thermal runaway of a lithium-ion pouch cell. A combination of high-speed operando tomography, thermal imaging and electrochemical measurements were used. The authors propose the layout of a sequence of events related to the evolution of voltage, temperature and chemistry of cell leading up to thermal runaway.

Region 1 (~5.1-5.3V): Caused is alleged to be the **irreversible heat generation** mechanisms such as ohmic losses which are most prevalent at high C-rates.

Region 2 (~5.4-5.5V): Initiation and progression of the **decomposition/formation of the SEI.**

Region 3 (~5.5V to 5.7V and back to 5.5V): Rise in voltage is caused by the resistance increase associated with the **gas pockets** forming between the active layers and the subsequent fall in voltage is due to decrease in resistance by the **bursting of the pouch** and the gases are channeled away.

Region 4 (~5.5V to 6.2V): The sharp maximum voltage is due to the **shutdown of the separator** and damage to the internal circuit caused by **rupture of cell.**

Batteries are constructed in a variety of shapes and sizes. Some common cell designs are cylindrical or prismatic cells. To form higher voltage batteries, the cylindrical cells are stacked in series and sealed together. Higher current can be obtained by increasing the electrode area, resulting in a larger diameter or longer length cell.A single cell that is wrapped by heavy outer plastic layers may create situations where ventilation is a concern. This condition worsens in large battery packs since the batteries are installed very close to each other in these packs. As one of the main degradation factors, overcharge occurs not only in a single cell, but also in battery packs where the cells are connected in series and there is a mismatch in their capacity. When these cells are used by the thousands such as in the case of a Tesla Model S vehicle, the large number of cells with even minor inconsistencies can easily accumulate significant heat.

As previously mentioned, every commercial battery comes with a certain set of specifications as recommended by the manufacturer for safe operation of the battery. According to the instructions of most battery manufacturers, the reliable operating temperatures required by a majority of current automotive lithium-ion batteries (graphite/$LiMn_2O_4$ or by acronyms C/LMO, $C/LiCo_xNi_yMn_zO_2$ or C/NCM, $C/LiFePO_4$

or C/LFP, C/$LiNi_{0.8}Co_{0.15}Al_{0.05}O_2$ or C/NCA) are: discharging at -20 to 55 °C and charging at 0 to 45 °C and for lithium-ion battery with $Li_4Ti_5O_{12}$ or LTO negative electrode, the minimum charge temperature can be -30 °C. Usually, the operating voltage of lithium-ion batteries is between 1.5 V and 4.2 V (C/LCO, C/NCA, C/NCM and C/LMO about 2.5-4.2 V, LTO/LMO about 1.5-2.7 V and C/LFP about 2.0-3.7 V) [42]. At this point, it is prudent to highlight an important fact. Batteries are constructed in a variety of shapes and sizes and their overcharge behavior is heavily dependent on the cell design and manufacturing processes. The varied electrode materials, cell manufacturers, solvent/electrolyte chemistries and basic cell type/design are all parameters that significantly affect the obtained results. Hence, despite the widely available literature on overcharge behavior of Li-ion cells, very little commonality is to be found.

CHAPTER III

ELECTROCHEMICAL ABUSE TESTING

Electrochemical Testing Protocols

There are several protocols that can be employed in order to gain information on the precise parameters of interest. Experimental testing of Li-ion cells requires significant time. Hence, unlike simulations which can be run repeatedly, it is of paramount importance that a Design of Experiments approach be employed when testing the cells so as not to drive up the cost and time taken to gain electrochemical information.

Formation Cycles

When fresh cells are obtained from any source, it is important to know their initial state in order to obtain reliable results. Therefore, before commencing any electrochemical tests, formation cycles should be applied to fresh ells. Formation cycles are usually done for anywhere between 1-5 times on a cell and are typically carried out at a low charging rate. These cycles also serve another function. When the cells are cycled at low charging rates initially, they allow a stable SEI layer to be formed within the cell. The importance of the SEI layer has already been addressed in the previous chapter. There are a few different types of formation cycles that have been used for the various sets of tests performed in this study and they are discussed below.

Constant Current Constant Voltage

Along with the voltage windows, recommendations for the charging protocol and temperature of operation are also provided by the manufacturer. For the NCR18650B cell used throughout this study, Panasonic recommends a Constant Current- Constant Voltage (CC-CV) charging protocol. A CC-CV protocol includes initially charging a cell up to the maximum safe upper voltage limit at a specified C-rate. This is the CC portion of the protocol. After the cell has reached the upper voltage, is charged at that constant voltage and allowed to continue charging until the current reaches a specified cut off lower limit. For the 18650 cells used here, the recommended charging protocol is to be performed as follow: CC charge at 0.5C up to 4.2 V and then CV charge it for a cutoff voltage of 50 mA at 25°C. Figure 6 shows the voltage, temperature and current behavior while charging a cell with the described CC-CV protocol. During the CC portion, the current remains constant while the voltage and temperature show a rise. During the CV portion of charging, the voltage of the cell remains constant while the temperature and current decrease. A CC-CV protocol is widely used in industry as well as academic arenas.

Constant Current Charge, Discharge, Charge (CC-CDC)

The CC-CDC protocol is another type of formation protocol that has been used in this study. This protocol is not a standard protocol. Hence the abbreviation CC-CDC is a term that been coined in house. This protocol includes charging, discharging and charging the cell again at a low charging rate of 0.1C. Therefore, henceforth when the CC-CDC protocol will be mentioned, it will be understood that the cell was first charged

at a constant rate of 0.1C up to 4.2 V (safe upper limit), discharged at 0.1C up to 2.5 V (safe lower limit) and charged again to 4.2 V at 0.1C.

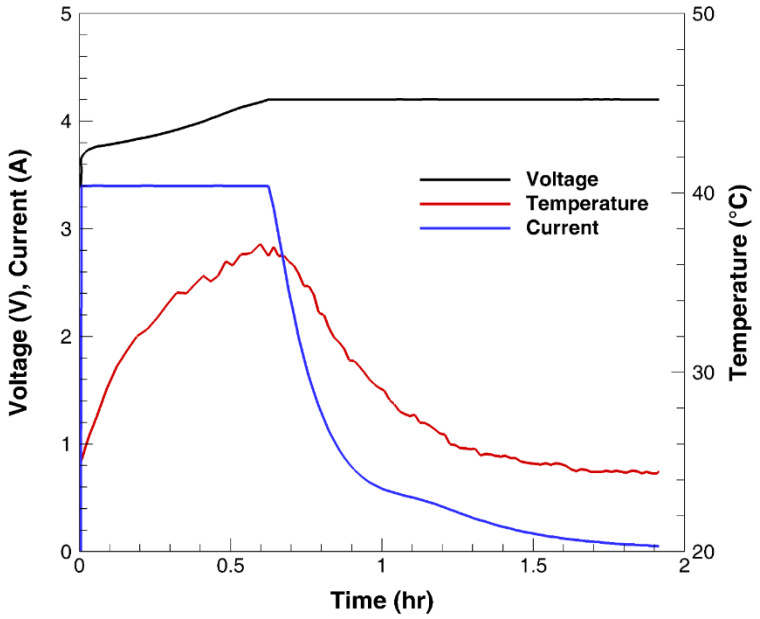

Figure 6 The voltage, current and temperature variables vs time are shown for a typical CC-CV protocol for a Li-ion cell charged up to 4.2 V.

There are no distinctive advantages or disadvantages to using one or the other protocol mentioned here. However, in the case of CC-CV protocol, the charging rate used was 1C which is higher than recommended and could pose a risk for a non-uniform and possibly degraded SEI. The formation cycles at 0.1C are better suited for the formation of a stable SEI. Figure 7 and Figure 8 show the variation in an overcharge test carried out with two different protocols. The maximum voltages before failure and temperatures reached during both the tests are the same. The difference in the protocols

is apparent in the time it takes for the cell to reach failure i.e. its path dependence. This shows that different protocols do not affect the end points of failure variables, but the variables show a path dependent overcharge profile.

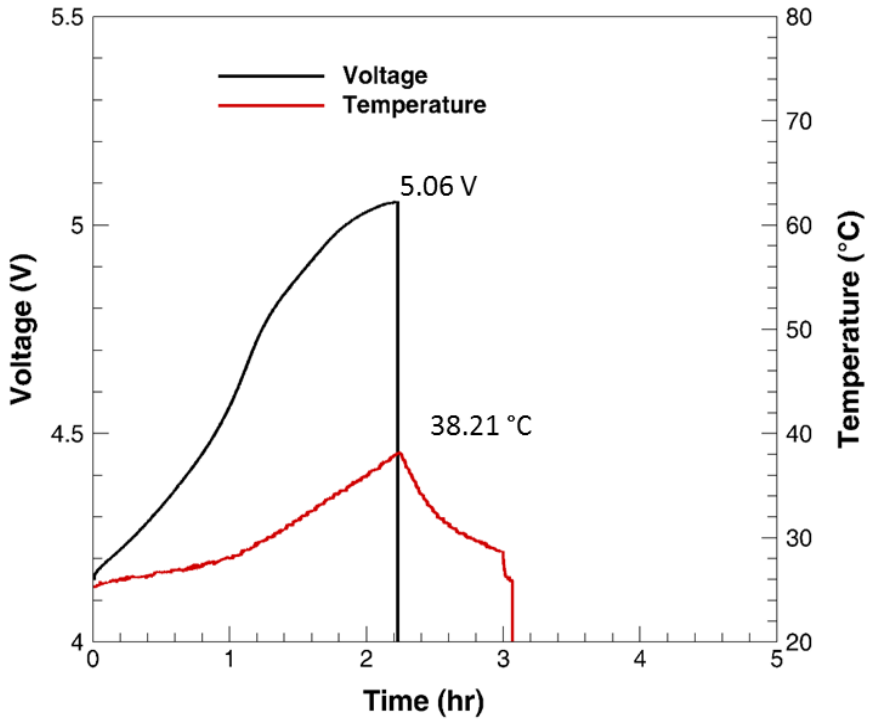

Figure 7 The voltage and temperature of a cell tested with a CC-CV (1C) protocol at C/10 overcharge up to the failure point. The maximum voltage reached is 5.06 V and the maximum temperature reached is 38.21 °C.

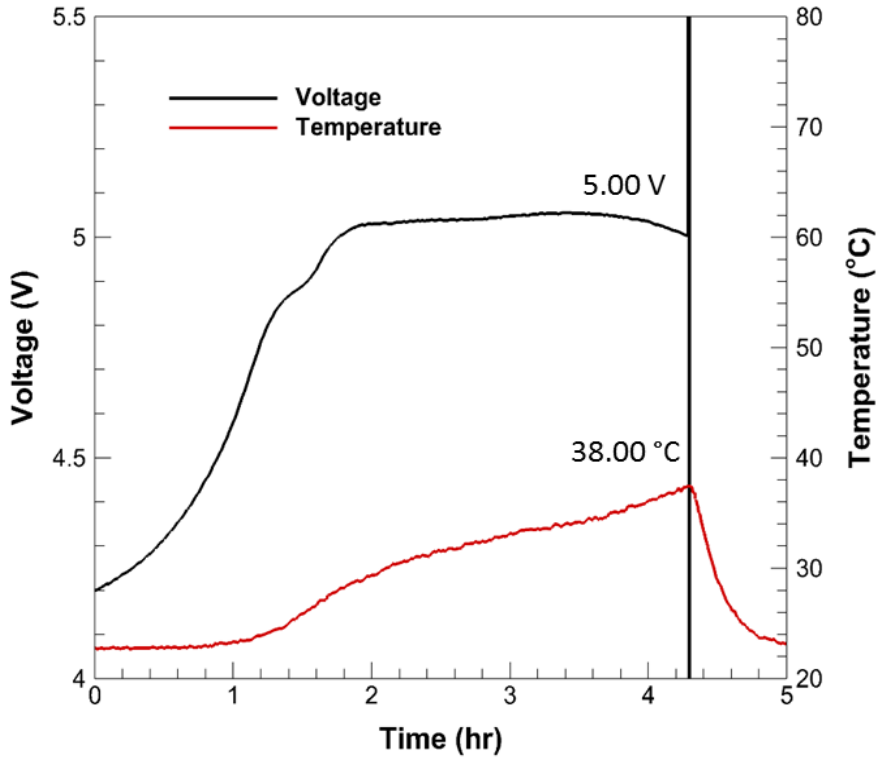

Figure 8 The voltage and temperature of a cell tested with a CC-CDC (C/10) protocol at C/10 overcharge up to the failure point. The maximum voltage reached is 5.06 V and the maximum temperature reached is 38.00 °C.

Effect of Cycling

Methodology

Overcharge is traditionally defined by the upper voltage limit of the particular cell and its chemistry. However, even if the manufacturer specifies an upper voltage limit, it may be possible that this limit has been set lower than necessary in order to have a margin of safety and protect the manufacturer from any possible liabilities in events of failure. In order to explore this further, overcharge tests were performed with four different upper voltages. Additionally, commercial secondary cells are not just for one time use. By

definition, these cells were invented so as to enable their continued use over a period of several hundred cycles. Hence, overcharge tests were performed by varying the upper voltage window and testing the cells over a period of 100 cycles. When the voltage of a cell is increased, the capacity that can be achieved from that cell also increases. In such a case, it may be tempting to charge a cell up to as high a voltage as possible and gain a larger amount of capacity from it. However, this scenario is not as straightforward. Even if a cell is charged to a high voltage and a large capacity may be gained for the first few cycles, it is highly likely that an increase in voltage limit will pose a threat to the cycle life of the cells. A set of tests performed in order to explore these factors are discussed below.

Cycling Test 1: For the overcharge stage of the testing protocol, the cell was first charged at 1C rate up to 4.2 V using a CCCV protocol with a cutoff current of 50 mA. After a brief resting period, the cell was charged again at 1C. This time the charging was done with the intent of overcharging the cell. The charging cycle was to be terminated when the cell reached 10 V or when the built-in protection mechanism of the 18650 cell became active.

Cycling Test 2: For the overcharge stage of the testing protocol, the cell was first charged at 1C rate up to 4.3 V using a CCCV protocol with a cutoff current of 50 mA. After a brief resting period, the cell was charged again at 1C. This time the charging was done with the intent of overcharging the cell. The charging cycle was to be terminated when the cell reached 10 V or when the built-in protection mechanism of the 18650 cell became active.

Cycling Test 3: For the overcharge stage of the testing protocol, the cell was first charged at 1C rate up to 4.3 V using a CCCV protocol with a cutoff current of 50 mA. After a brief resting period, the cell was charged again at 1C. This time the charging was done with the intent of overcharging the cell. The charging cycle was to be terminated when the cell reached 10 V or when the built-in protection mechanism of the 18650 cell became active.

Cycling Test 4: For the overcharge stage of the testing protocol, the cell was first charged at 1C rate up to 4.2 V using a CCCV protocol with a cutoff current of 50 mA. After a brief resting period, the cell was charged again at 1C. This time the charging was done with the intent of overcharging the cell. The charging cycle was to be terminated when the cell reached 10 V or when the built-in protection mechanism of the 18650 cell became active.

Results and Discussion

The voltage vs. capacity of each cell was acquired. Figure 9 is a graph of the charge discharge voltage and capacity of the Cell 1 tested up to 4.2 V. The nominal capacity of the NCR18650B cell is 3.4 Ah. It is evident that this cell tested at 1C and charged discharge for 100 cycles shows some capacity fading at the end of the 100^{th} cycle. In the first cycle, the capacity obtained was 2.5 Ah. As the cell was progressively cycles, the capacity reduced. After 50 cycles, the capacity decreased to 1.34 Ah and after 100 cycles, the capacity decreased further to 0.5 Ah. This also sheds light on the fact that charging rate is an important factor in capacity fade of the cells. If the cells had been cycled at the manufacturer recommend rate of 0.5C, the capacity fade noticed would have been lesser than that observed here.

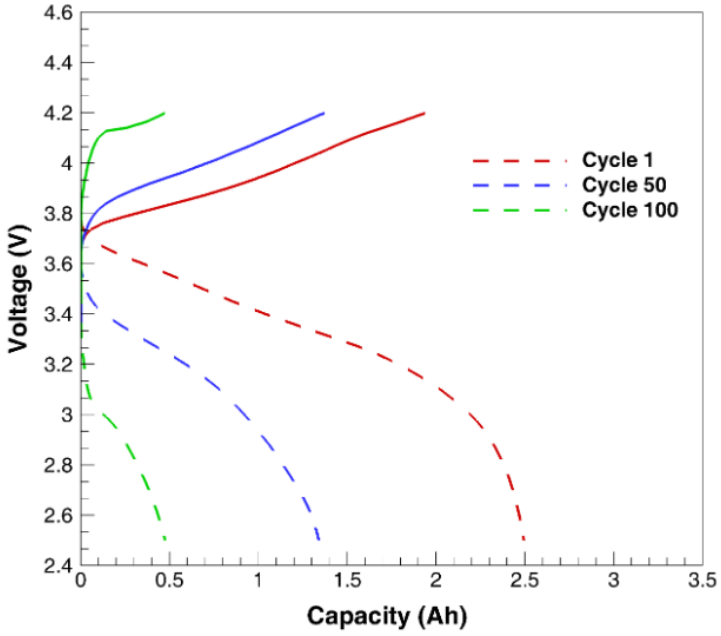

Figure 9 Comparison of the capacity fade noticed for a Li-ion cell cycled at 1C for 100 cycles up to 4.2 V. The voltage vs. capacity behavior for the 1st, 50th and 100th cycles is depicted.

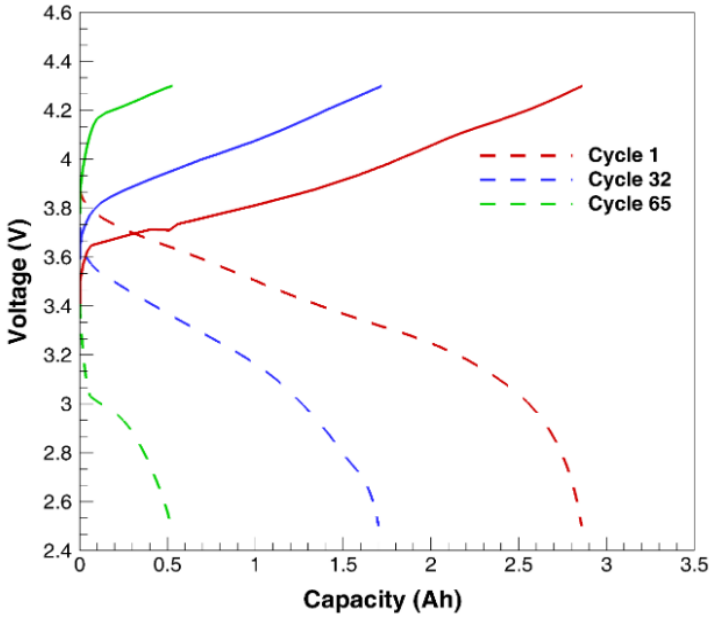

Figure 10 Comparison of the capacity fade noticed for a Li-ion cell cycled at 1C for 100 cycles up to 4.3 V. The voltage vs capacity behavior for the 1st, 32nd and 65th cycles is depicted.

Figure 10 is a graph of the charge discharge voltage and capacity of cell 2 tested up to 4.3 V. The voltage and capacity behavior of this cell is as expected. The capacity achieved at the 1st cycle is 2.89 Ah, at the 32th cycle is 1.7 Ah, and at the 65th cycle is 0.5 Ah. Even though the capacity at the first cycle was higher as compared to Cell 1, the subsequent capacity fading after 100 cycles is worse than for the cell tested at 4.2 V. Another key observation is that the reason this graph doesn't show the same 1, 50 and 100 cycles is because the cell could not withstand overcharge cycling for 100 cycles and failed after the 65th cycle.

The next cell tested was cell 3 up to 4.4 V. As might be expected, as the voltage window was increased, the cell capacity obtained was also higher. In this case, when the cell was charged up to 4.4 V, the capacity observed for the 1st cycle was 3.15 Ah. This is much higher than that observed for the previous two cells. The cell failed at even lower cycles than the previous cells. This cell was able to cycle for 44 cycles after which the internal protection of the cell was activated and it could not be charged any more. The capacity observed during the first cycle was 3.15 Ah, during the 22nd cycle was 2.3 Ah and for the last cycle was 0.78 Ah. This overcharge cycling behavior is depicted in Figure 11.

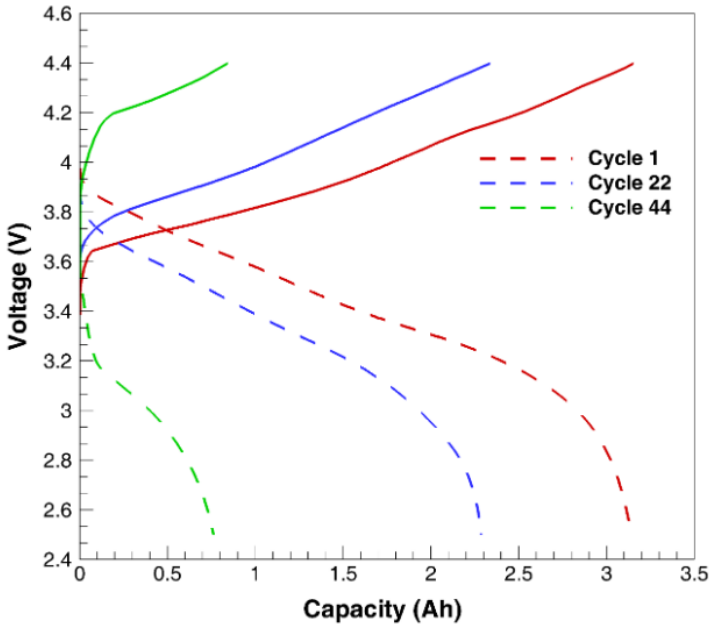

Figure 11 Comparison of the capacity fade noticed for a Li-ion cell cycled at 1C for 100 cycles up to 4.4 V. The voltage vs capacity behavior for the 1st, 22nd and 44th cycles is depicted.

The last cell tested in this set of tests was cell 4. This cell was CC-CV charged at 1C up to 4.5 V and the voltage vs capacity behavior was observed. It can be seen that this cell was capable of delivering the highest charge discharge capacity among all the cells tested. The capacity of 3.2 Ah achieved in this cell was closest to the nominal capacity of the cell (3.4 Ah). Since the voltage window of this cell was extended to a higher limit than those of the previous cells, it was expected that this cell would deliver the maximum amount of capacity and this can be verified from the cell behavior in Figure 12.

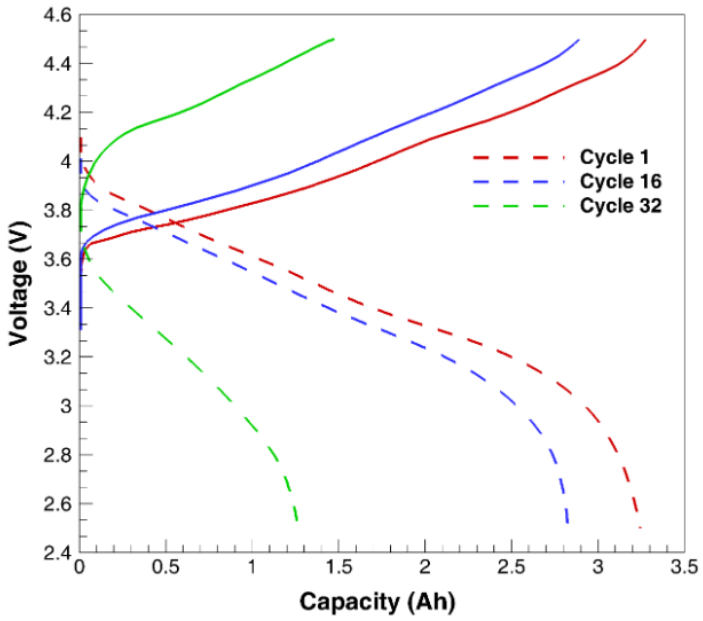

Figure 12 Comparison of the capacity fade noticed for a Li-ion cell cycled at 1C for 100 cycles up to 4.5 V. The voltage vs capacity behavior for the 1st, 16th and 32nd cycles is depicted.

This cell failed the earliest after only 32 cycles of overcharge. Hence, the capacity fade noticed in this cell was the largest as compared to other cells. In order to compare the capacities of the four cells achieved after cycling, the capacity retention of the four cells was graphed and is shown in Figure 13. Even though the cell charged up to 4.5 V has capacity retention of 38.93%, it fails very quickly as compared to the other cells. Cells 1 and 3 tested at 4.2 and 4.4 V respectively have comparable capacity retention; however, there is a significant mismatch in the number of cycles leading up to cell failure.

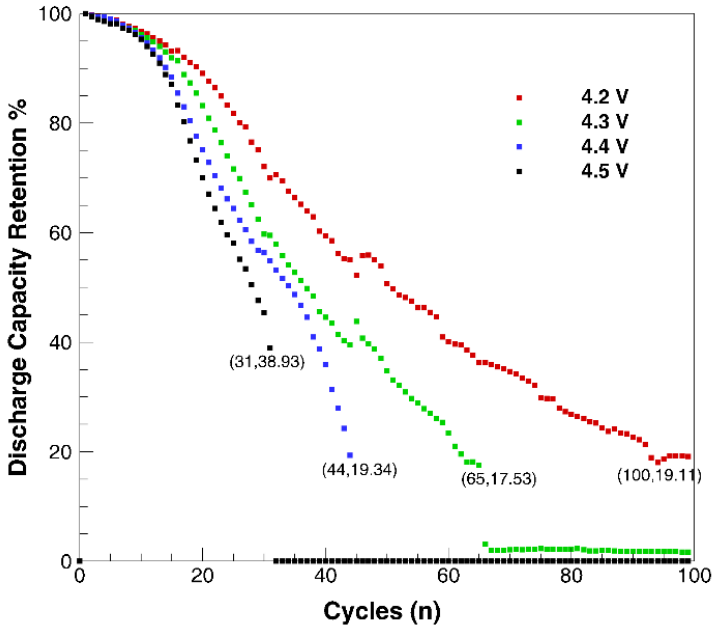

Figure 13 Discharge capacity retention of four cells overcharged to 4.2, 4.3, 4.4 and 4.5 V and tested over a period of 100 cycles.

In conclusion, it is emphasized that while increasing the voltage of a cell during charging may provide higher capacity which is a desirable quality; it may also lead to cell degradation quicker than normal and can significantly reduce the cycle life.

When the capacity of a cell changes during testing, it signifies a change occurring inside the cell. This concept is especially helpful when elucidating the overcharge behavior of cells because it helps to identify the times, states of charge, and possible reactions within the cell that cause it to reach failure. A popular method for capturing this behavior is differential (voltage, capacity) analysis. In this case, a

differential capacity with respect to cycle number was performed. The graph shows a dQ/dN analysis on the four cells tested at 4.2, 4.3, 4.4 and 4.5 V.

Overall, it is seen that there are several peaks in the differential capacity behavior. Some of these peaks can be simply noise. However, in the curves for each cell, there are three major peaks that are common to each cell regardless of the upper voltage they were tested to. This dQ/dN analysis can therefore serve as a potential indicator that at the major peaks indicated, there are changes happening in the cell. These indicators can aid researchers in exploring these particular times during cell overcharge and help to isolate potential reasons that lead up to overcharge cell failure. At the very least, even if the reasons for this overcharge behavior are not deciphered, these results can provide a kind of alert about the hazardous events happening at these points. The curve for 4.2 V shows similar peaks as the rest, but upon cursory inspection, the intensity of the peak for 4.2 V appears to be lower or more 'benign'. This is to be expected since by definition, charging the cell up to 4.2 V is not considered to be an overcharge. It is interesting to note how the peaks for the remaining three cells are similar; they only seem to differ in the intensity of the peaks perhaps and of course, the number of cycles before cell failure.

Effect of Charging Rate

Methodology

The various parameters that can be manipulated during overcharge testing include protocol, upper voltage limit, and charging rate. The effects of protocol and upper voltage limit have been discussed in the previous two sections. Naturally, the next thing to follow is the investigation of the effect of charging rate on the overcharge of a

commercial Li-ion 18650 cell. It is prudent to keep in mind that overcharge behavior is extremely sensitive and heavily dependent on the cell chemistry. Therefore, the overcharge behavior observed in this section of tests may not necessarily coincide with tests performed with different cell chemistry.

Overcharge Test 1: A CC-CDC formation protocol (C/10) was applied to this cell before commencing the overcharge. For the overcharge stage of the testing protocol, the cell was discharged at C/10 up to 2.5 V, charged at C/10 up to cell failure. The charging cycle was to be terminated when the cell reached 10 V or when the built-in protection mechanism of the 18650 cell became active.

Overcharge Test 2: A CC-CDC formation protocol (C/10) was applied to this cell before commencing the overcharge. For the overcharge stage of the testing protocol, the cell was discharged at 1C up to 2.5 V, charged at 1C up to cell failure. The charging cycle was to be terminated when the cell reached 10 V or when the built-in protection mechanism of the 18650 cell became active.

Overcharge Test 3: A CC-CDC formation protocol (C/10) was applied to this cell before commencing the overcharge. For the overcharge stage of the testing protocol, the cell was discharged at 2C up to 2.5 V, charged at 2C up to cell failure. The charging cycle was to be terminated when the cell reached 10 V or when the built-in protection mechanism of the 18650 cell became active.

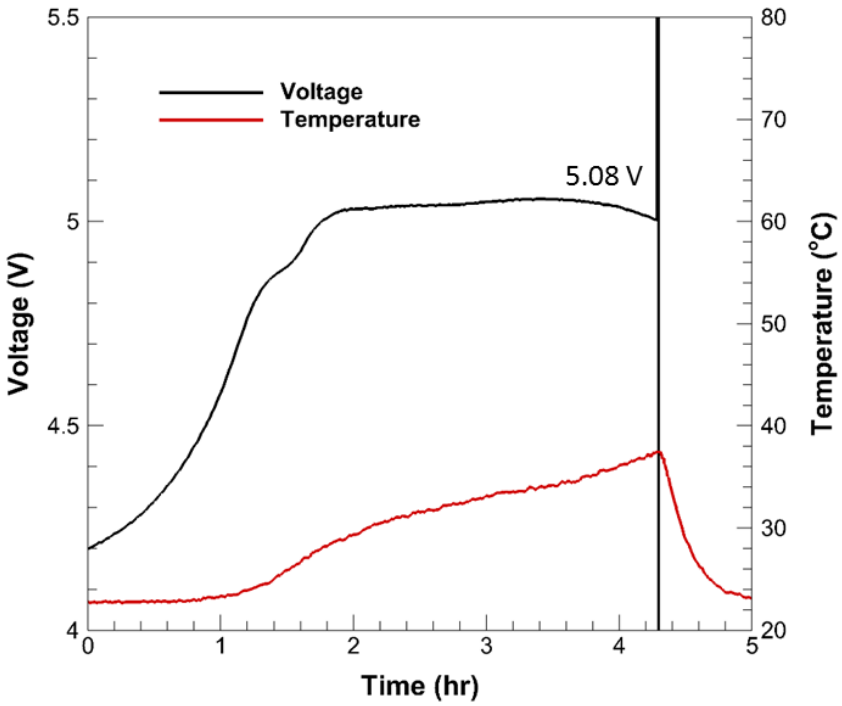

Figure 14 Voltage, temperature vs. time curves for a cell overcharged at a rate of C/10 using the CC-CDC formation protocol and overcharge test protocol describe in overcharge test 1.

The voltage and temperature vs. time curves are shown in Figure 14 for the cell overcharged at a C-rate of 0.1C. The time it took for the cell to reach failure which is defined as the point where the internal protection of the cell is activated was approximately 4 hours. This time is not the total test time, rather it is the time taken for the cell to overcharge from 4.2 V up to failure. As is seen from the graph, with the progression of time, the voltage and the temperature of the cell also increased. The maximum voltage reached by this cell was 5.08 V and the maximum temperature was 38

°C. After failure, the current applied to the system immediately falls down to 0. As soon as the input of current is terminated, the temperature rise also stops and the cell starts to cool down. This result is important because it is not observed for all the charging rates. This leads to the hypothesis that the exothermic reactions occurring in the cell are particularly dependent on the C-rate.

Figure 15 is a similar graph for the cell overcharged at 1C. The maximum voltage of the cell was 5.15 V before failure. The maximum temperature in the cell was 53.18 °C. Both the temperature and voltage are higher than that seen in the cell overcharged at 0.1C. It is a very interesting phenomena that the temperature continued to rise for a few seconds even after the cell had reached failure and the current had fallen down to zero. This implies that, even for a few seconds, there were exothermic reactions occurring in the cell which accelerate the temperature of the cell and continued to occur for a short time even after cell failure. The time taken for the cell to reach overcharge after 100% SOC was approximately 25 minutes. As expected, since the charging rate was higher, the time taken for the cell to overcharge was lower.

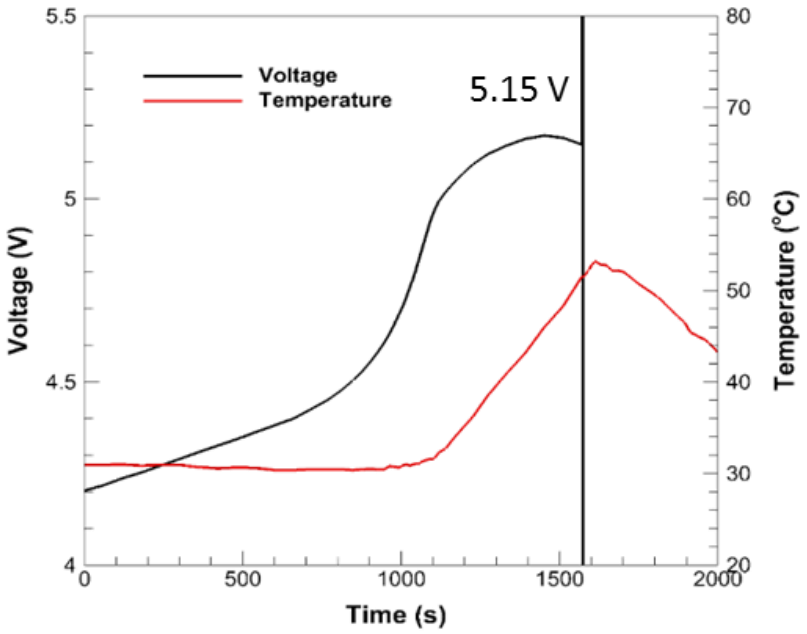

Figure 15 Voltage, temperature vs. time curves for a cell overcharged at a rate of 1C using the CC-CDC formation protocol and overcharge test protocol describe in overcharge test 2.

Figure 16 shows the voltage and temperature curves for the last cell tested in this group. This cell was overcharged at 2C and it took approximately 15 minutes for the cell to fail during overcharge. As compared to the previous cells, this cell of course failed the fastest due to the higher charging rate. One might expect that a trend in voltage and temperature may have emerged when observing the results from previous two tests. However, this was not the case. The maximum voltage reached in this test was 5.13 V which is comparable (but slightly lower) than that observed for the cell charged at 1C. It was expected that the voltage with this cell would be the highest in accordance with its high C-rate. Similarly, the maximum temperature in this test was 45.69 °C. Unexpectedly, this was again lower than that for 1C. The protocol for the 2C test was set

in such a way that the temperature would be kept on recording even after the cell had failed. However, due to the safety instructions built in to the electrochemical test equipment ARBIN, the data collection of the test was automatically stopped by ARBIN due to unsafe voltage detection by the system. Unfortunately, comments about the rise of temperature after the cell has reached failure for 2C cannot be made at this time due to the unavoidable circumstance.

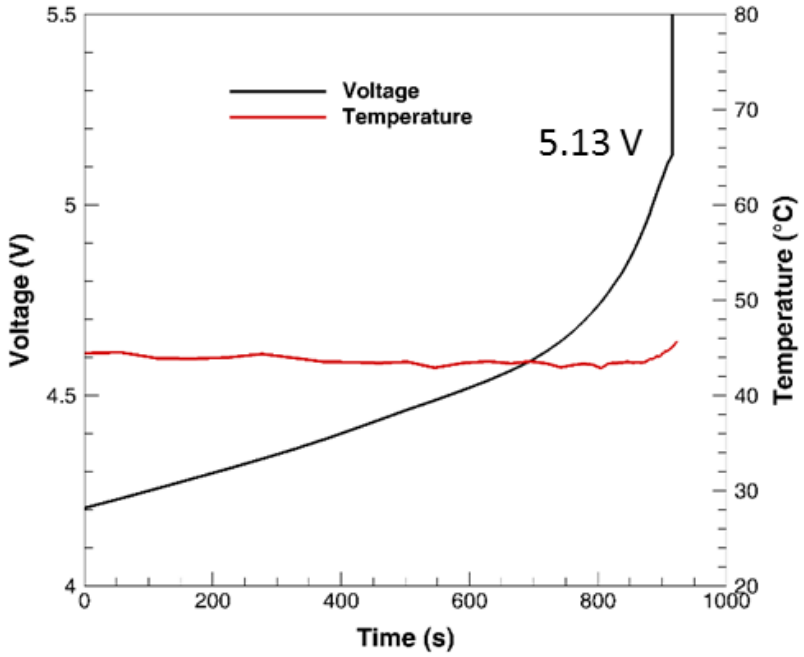

Figure 16 Voltage, temperature vs. time curves for a cell overcharged at a rate of 2C using the CC-CDC formation protocol and overcharge test protocol describe in overcharge test 2.

With the increase of C-rate, it was initially expected that the maximum voltage and temperature achieved in the cell would also increase. However, such a straightforward trend was not observed. The cell overcharged at 1C showed the highest

voltage and temperature, followed by the cell overcharged at 2C and finally, the cell overcharged at C/10 showed the lowest temperature and failure voltage. These trends were initially thought to be erroneous, but in fact, based on further post-mortem analysis, a suitable reasoning was found. This will be explained in the next chapter.

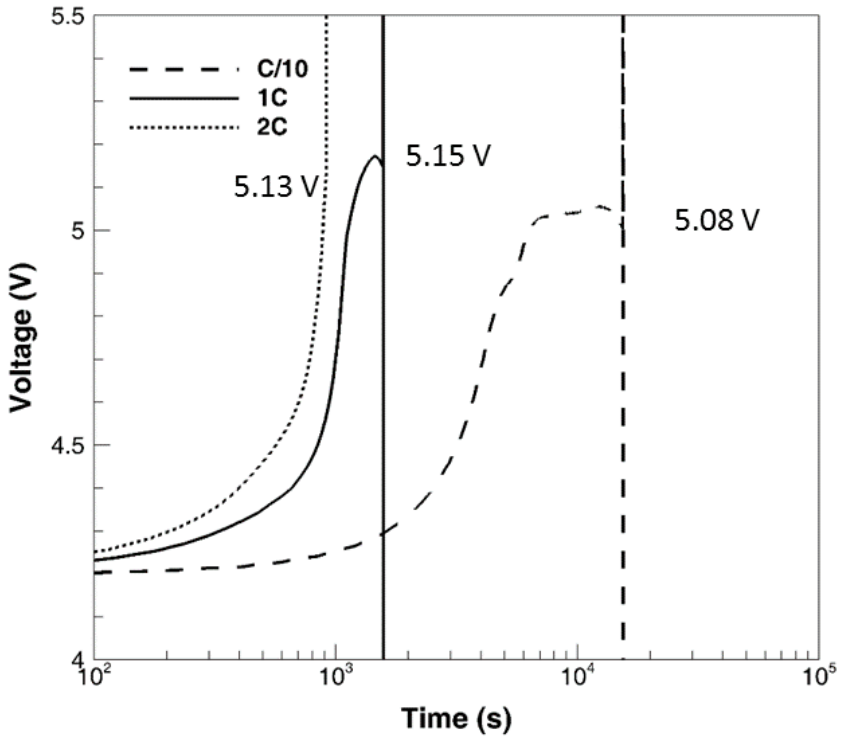

Figure 17 A comparison of the maximum voltages achieved before failure in cylindrical Li-ion cells during overcharge. The cell charged at 1C showed the highest voltage, followed by the cell charged at 2C and finally, the cell charged at 0.1C.

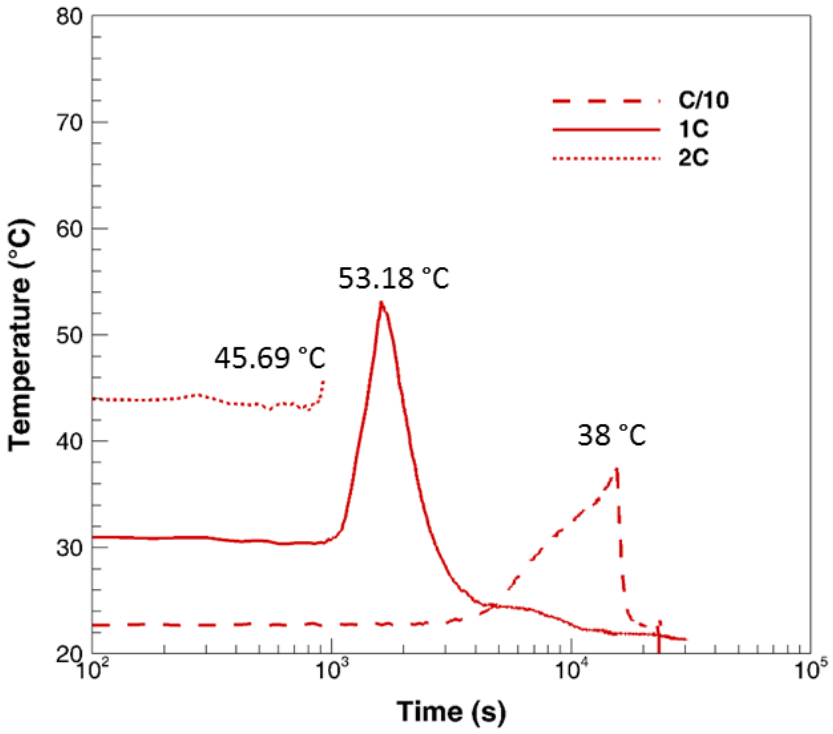

Figure 18 A comparison of the maximum temperatures achieved before failure in cylindrical Li-ion cells during overcharge. The cell charged at 1C showed the highest temperature, followed by the cell charged at 2C and finally, the cell charged at 0.1C.

Electrochemical Impedance Spectroscopy

Overcharge performance of two Li-ion cells was studied using electrochemical impedance spectroscopy (EIS). Impedance is the measure of the ability of a circuit to impede the flow of electrical current. Specifically, it refers to the dependent resistance to current flow of a circuit element. In order to conduct this test, a small sinusoidal potential or current of fixed frequency is applied and the response is measured and impedance is measured at each frequency. The changes in the impedance of the cell and its components based on their state of charge were tracked. To ensure the stable and

complete formation of the solid electrolyte interphase, the cells were subjected to formation cycles via the CC-CDC protocol at C/10.

EIS Test: After the second charge, the cell was discharged at a low C-rate of 0.04 corresponding to C/25. This C-rate is chosen so as to best replicate the Open Circuit Voltage (OCV) profile of the cell. After this discharge, the cell is subjected to the final charge cycle. This charge cycle is also done at C/25 and within this stage, there is no upper cutoff voltage specified and the cell is allowed to overcharge until failure. During this protocol, EIS measurements were taken every 5 hours during C/25 discharge duration (between 4.2 - 2.5 V) and every 1 hour during overcharge.

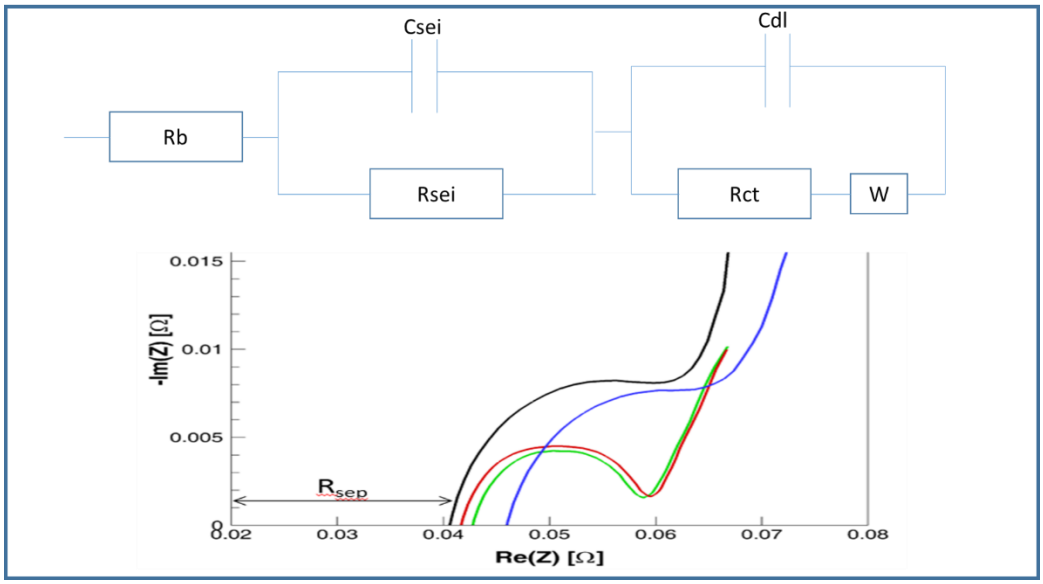

Figure 19 Typical EIS of the Li-ion cell and the regions showing various sources of resistance in the cell. Inspired and redrawn based on [45].

Results and Discussion

In most of voltage range, the EIS of Li-ion cells is composed of two partially overlapped semicircles and a straight sloping line at low frequency end known as the tail. Such a pattern of the EIS can be fitted by an equivalent circuit shown in inset of Figure 19. The R_b is bulk resistance of the cell, which reflects electric conductivity of the electrolyte, separator, and electrodes; R_{sei} and C_{sei} are resistance and capacitance of the solid-state interface layer formed on the surface of the electrodes, which correspond to the semicircle at high frequencies; R_{ct} and C_{dl} are faradic charge-transfer resistance and its relative double-layer capacitance, which correspond to the semicircle at medium frequencies (not seen in the EIS behavior above); W is the Warburg impedance related to a combination of the diffusional effects of lithium ion on the interface between the active material particles and electrolyte, which is generally indicated by a straight sloping line at low frequency end. The combination of R_{ct} and W is called faradic impedance, which reflects kinetics of the cell reactions. Low R_{ct} generally corresponds to a fast kinetics of the faradic reaction [45].

The voltage window in the cell tested at C/25 is shown in Figure 20. The cell was discharged up to 2.5 V and allowed to charge past 4.2 V up to failure, which happened at 5.0 V for this cell. The corresponding EIS plot in the overcharge region of the cell is shown in Figure 21. A 100% SOC is defined at the point where the cell has reached full capacity. Beyond the 4.2 V upper limit, the EIS data for the cell was recorded every one hour up to failure. In Figure 21, the EIS curves at 111% and 134% SOC are shown. Both the curves have a similar shape – one semi-circle which corresponds to the charge

transfer region and the sloping tail which is indicative of the diffusion phenomena in the cell. The first semicircle corresponding to the SEI region is not visible which is indicative of an SEI layer degradation phenomena happening inside the cell.

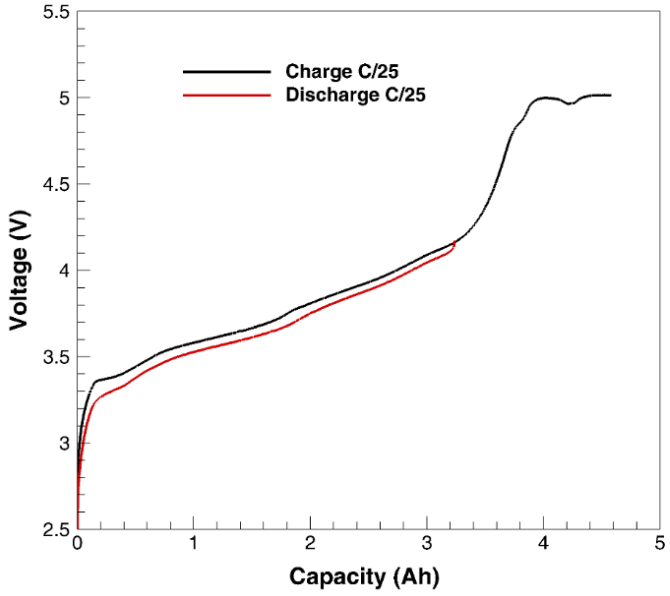

Figure 20 The charge and discharge voltage vs. capacity curves for the cell tested with the CC-CDC formation cycles and overcharged at a rate of C/25. The maximum voltage at failure is 5.0 V.

Additionally, the major difference seen is that, with the progression of overcharge, the impedance arising due to the separator is seen to be increasing. This is indicative of the activation of separator shutdown mechanism inside the cell. As was discussed before, separators are manufactured with shutdown properties in order to protect the cell and that is what is observed during this test. Therefore, it is evident that

electrochemical impedance spectroscopy is a very useful technique in extracting the relation between the stability of cell components and their state of charge.

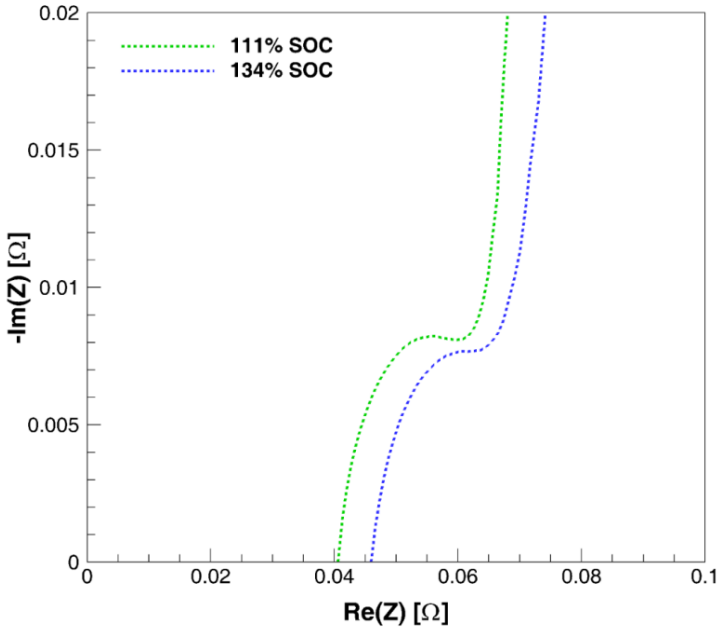

Figure 21 Electrochemical impedance spectroscopy graph of the Li-ion cell tested at C/25. The curves show the impedance development in the cell during the overcharge region.

While EIS may have given the potential causes contributing to or occurring during overcharge of a cell, a well performed post mortem analysis can provide confirmation of the findings from electrochemical measurement techniques. The next chapter describes the destructive physical analysis performed on several cells, the process used for the disassembly of the cells, and the information that was gained through visual inspection of every component within the cell after overcharge failure.

CHAPTER IV

DESTRUCTIVE PHYSICAL ANALYSIS

Internal Structure of the Cell

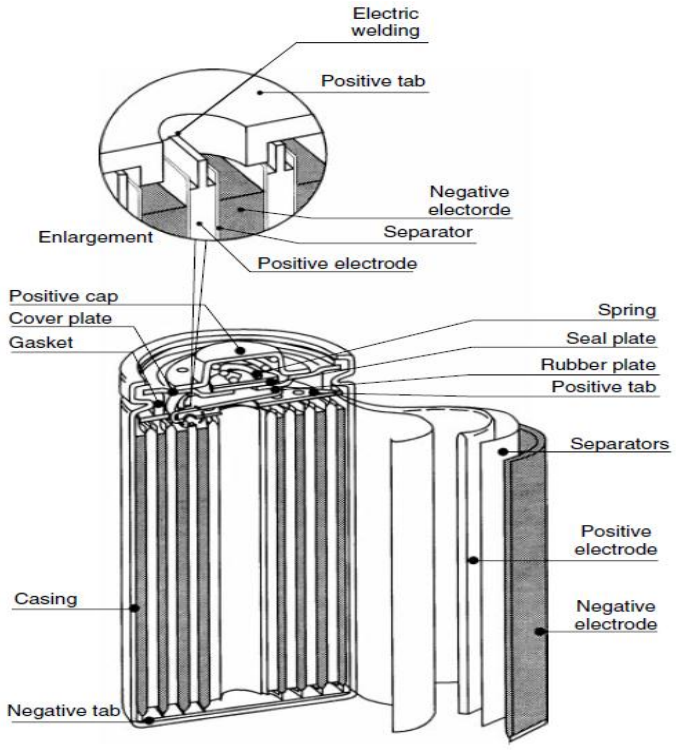

*Figure 22[1] A schematic of the intenal structure and layout of components of a cylindrical Li-ion cell. Some of the layout of cylindrical cells may vary depending upon the manufacturer [46]**

The batteries investigated in this work at the commercial Li-ion 18650 type cylindrical batteries manufactured by Panasonic. Many published works utilize post mortem analysis as an invaluable tool for obtaining additional insights into the thermal stability and failure behavior of Li-ion cells. The standard 18650 type batteries have dimensions

[1] Reprinted with permission from "Practical Batteries" in *Handbook of Battery Materials**, Nishio, K. and N. Furukawa, 2011, Wiley-VCH Verlag GmbH & Co. KGaA.

of 1.8 cm diameter, 6.5 cm length and are wound in a spiral jelly-roll type configuration. The structure of the battery can be classified into two main categories: the body along with current collectors and the safety protection mechanisms. The design of a Panasonic Li-Ion cylindrical cell is shown in Figure 22.

Outer Casings

Starting from the outer most layers and working inwards, the first thing seen on a cell is the plastic wrapping on which the cell type, manufacturer and other information is printed. Commercial cells today are available with or without tabs. If bought without tabs, the tabs can be attached later on when needed by spot welding.

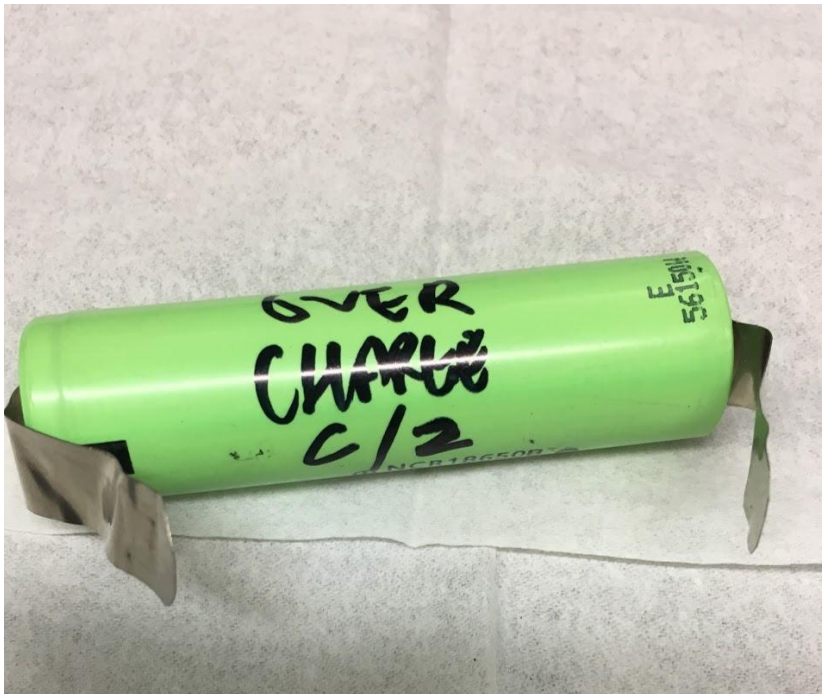

Figure 23 A Panasonic NCR 18650 cell ready to be opened for post-mortem analysis. This cell is placed on a non-metallic surface in order to avoid short cicruit of the cell.

Figure 24 The cell housed in a metal can is visible after removal of the outer palstic layer of the cell.

The next layer to be seen once the plastic is removed is the aluminum can and the header attached to it as shown in Figure 24. The aluminum can is a feature missing from the prismatic type or pouch cells. While the absence of the can provide pouch cells with higher gravimetric density, it also is the reason swelling and gassing is a constant safety issue in Li-ion pouch type cells. The aluminum can in the cylindrical cells provides a measure of physical protection against swelling and distortion. Once the can and the header are cut, a clear view of the cell header and its attachment to the cell body is visible as shown in Figure 25.

Figure 25 The cell header is cut with a can cutter in order to expose the header and the the main body of the cell. The two parts are connected by the positive tab.

Cell Header Components

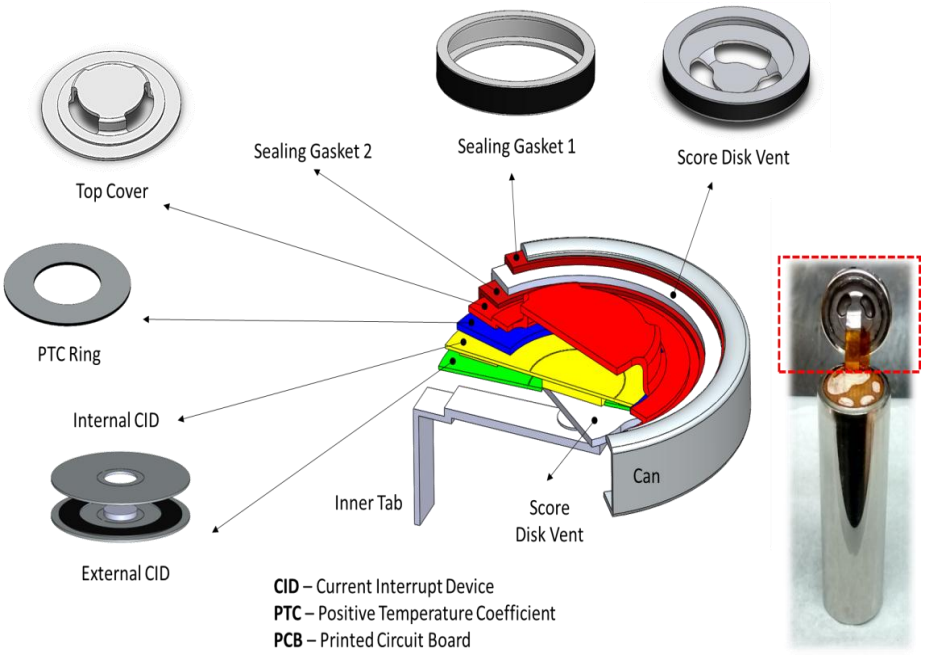

Figure 26 An exploded view of the cell header and its components. Several safety deatures installed in the cell are visible in this view.

The first and outermost component of a cell header is an external metallic can in which the rest of the components are fitted. Below the can is a layer of gasket which ensures a proper seal. The gasket is made up of an insulating material which doesn't allow the passage of electricity between the positive and negative terminals. The next layer is a score disk vent. This is one of the protection mechanisms that were described in a previous section. The vents allow gases to escape from the cell in case of excess pressure build up. Vents are usually employed as a backup device and not as a primary source of

cell protection. Below this, another sealing gasket is layered. Below this gasket, the top cover or the positive terminal is installed. The positive terminal protrudes from the top of the battery and is made of stainless steel. The positive terminal of the cell is connected to the positive terminal of the device to be powered. The next component is the Positive Temperature Coefficient protective device. When an over-current situation occurs in the cell, the excess heat travels through the PTC causing the material in it to undergo a phase change and expand. Cylindrical type cells have a PTC employed in the sealing cap which serves as a protective mechanism. Below the PTC is another protective measure known as the Current Interruption Device (CID). The CID is a two component assembly. A top cover (shown in Figure 26 as the internal CID) is assembled on top of a lower disk. The top disk is flat while the lower disk consists of a domed metallic protrusion. Any event in the cell that causes the internal pressure to increase will cause the activation of the CID. On activation, the top disk of the CID will disconnect from the lower just enough so that there is a physical break between the jelly roll and the positive terminal. This is a more extreme form of protection because once activated, the CID renders the cell unusable.

Figure 27 A comparison between an activated and a non-activated current interruption device of a cylindrical Li-ion cell.

A fractionally open gap as seen in the activated CID of Figure 27 is the indicator that the contact in the cell was broken. Finally, the last component connecting the cell header to the jelly roll is the positive tab. Often, if the cell is abused, a pool of electrolyte can be seen on top of and around the insulation plate. There are two insulation plates installed in a cell. One of the plates is situated at the top of the roll between the roll and the cell header as seen in Figure 28. Another insulation plate is installed in a similar configuration at the bottom of the cell between the bottom of the jelly roll and the can.

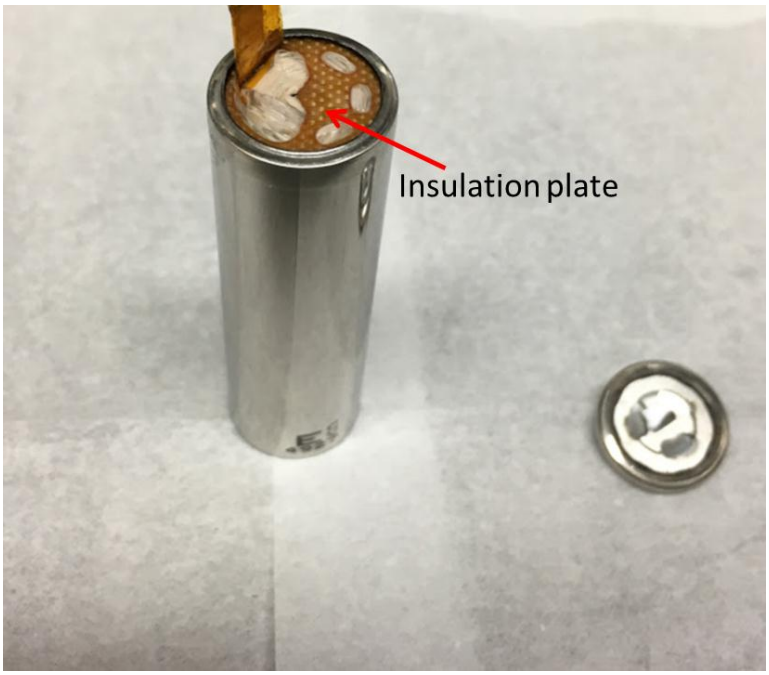

Figure 28 An exposed insulation plate is visible in a cylindrical Li-ion cell after the cell header as been separated from the body.

Once the external can is cut open, the electrode materials in the jelly roll format become visible. A tape holds the electrodes in a spiral configuration as well as the negative lead that connects to the negative electrode. This set up is visible in Figure 29.

Once the tape and the tab are removed, the electrodes can be separated. The battery is fabricated from four layers of material that are rolled up to form a cylinder in what is known as the 'jelly-roll' configuration as seen in Figure 30. The layers are the positive electrode, separator, negative electrode, and then a second separator. First, a separator sheet is laid down over which the negative electrode is layered. Next, the second layer of separator is laid down which acts as a physical barrier between the negative and the positive electrode. The positive electrode is then laid on the previous

three layers and the sheets are then wound tightly around a thin metal tube called the mandrel.

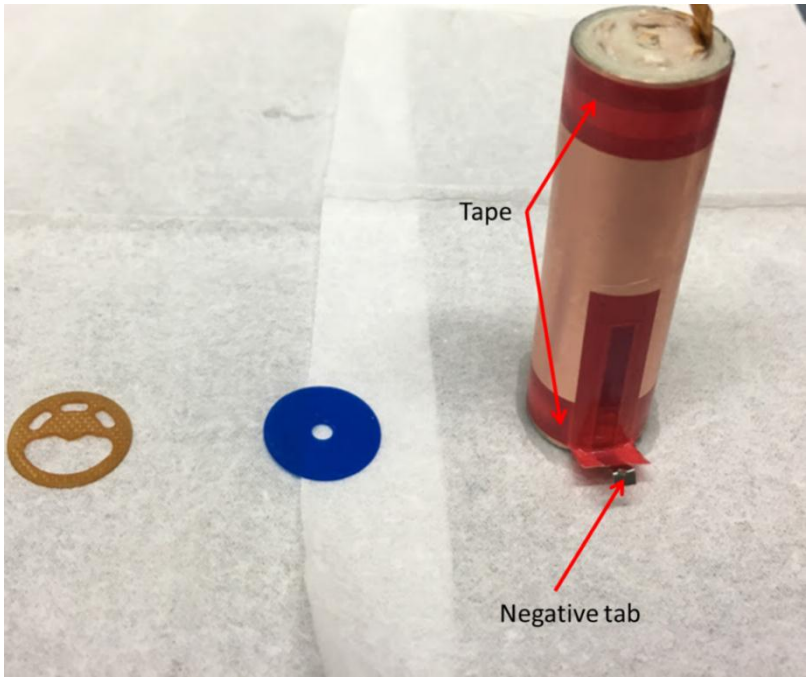

Figure 29 The internal structure of the cell as exposed after the metallic can housing the jelly roll has been cut. At this stage, the insluation plates and the negative tab are visible.

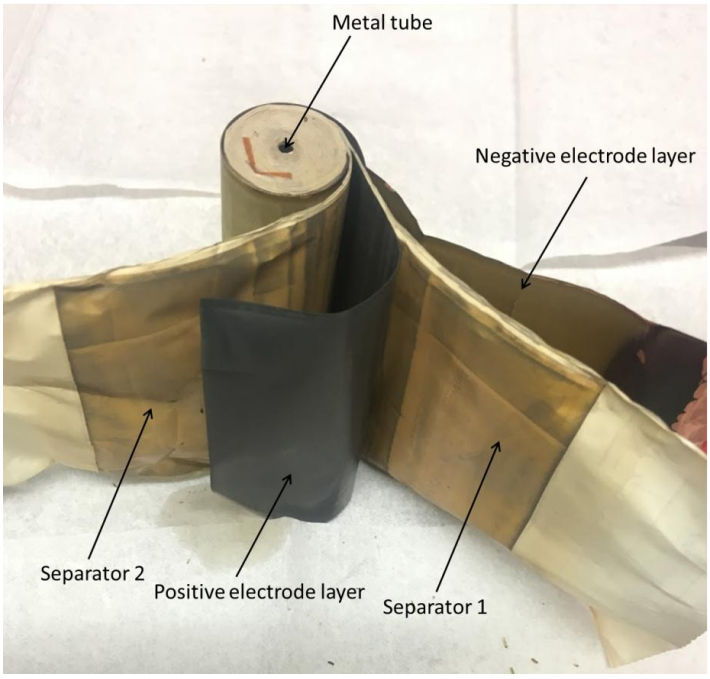

Figure 30 The jelly roll type of configuration is seen of a cylindrical Li-ion cell. The anode, cathode and the two separators that segregate them are visible at this stage of DPA.

The positive electrode material of an NCR18650B type cell is made of Lithium Cobalt Nickel Aluminum Oxide abbreviated as NCA. The negative electrode material used in this cell is graphite C. An aluminum foil which is resistive toward the oxidizing potential is used as the current collector for the cathode (positive electrode). Similarly, a copper current collector resistive to a reducing potential is used on the anode (negative electrode side). In the figure above, a portion of the copper current collector can be seen attached to the anode. The precise separator material used in this cell is not disclosed in the official product information sheet.

Cell Disassembly

Safety

Upon closer inspection, the casing of every cell comes equipped with a warning from the manufacturers advising against the disassembly of the cell. Lithium-ion cells are equipped with a plethora of hazards and disassembly of these cells should be avoided. Inadvertent short circuiting of the cells is one of the most prominent dangers of opening a li-ion cell as it may lead to lab fires if not brought under control. Disassembly of fully charged cells is an even more extreme condition as the energy of the system is very high at that point. However, aims of certain works (such as this one) almost mandate the need for a post mortem inspection of the cells in order to gain crucial information. In such a case, disassembly must be performed only by seasoned experimenters and even then, every ounce of utmost precaution is advised. Furthermore, the inclusion of toxic materials in the cells exponentially increases the risk of health hazards during disassembly.

Procedure

1. Preparation of materials – Four Ziploc bags are taken and labeled according to the components they will house. Two bags will contain one electrode each, another bag will contain the two separators and the last bag will be utilized to gather any other cell components of interest such as the cell header.
2. Glove box cycling – Some components of Li-ion cells can react violently with the moisture or oxygen present in the atmospheric air. Hence, disassembly must always be done in an inert atmosphere such as a glove Box. The glove box used

during this study contained of a highly inert atmosphere filled with Argon gas. The lowest levels of 0.5 ppm hydrogen and oxygen gas contamination were accepted. The materials such as the plastic bags, the cell, and any photographic equipment needed are all inserted in the antechamber tray and firmly locked into place. Care is taken to ensure that the plastic bags are opened before inserting them in the glove box so that the air inside them can be completely removed. The antechamber works on a two way valve system. First, all the air that was introduced into the antechamber is removed thereby putting it in vacuum. This is allowed to be done for approximately 3 minutes. The valve is now turned so that the chamber can be slowly flushed with the Ar gas. This is also done for 3 minutes. This procedure is repeated for a total of two times thereby ensuring the least possible contamination. Figure 31 is a picture of the glove box used for the experiments which is installed at the Energy Transport Sciences Laboratory.

Figure 31 The glove box used for this research study as installed in the Energy and Transport Sciences Laboratory at Texas A&M University, College Station, TX.

3. Transfer of materials – The antechamber is opened inside the glove box and the materials are placed on the floor of the box. Before beginning the disassembly, care is taken to place any kind of nonmetallic material on the surface over which the cell will be opened. The metallic floor of the glove box poses a threat for short circuit of the cell due to unintentional contact of the external tabs.
4. Removal of tabs – The tabs of the cell are removed with a pair of narrow tipped pliers and placed in a plastic boat available inside the cell.

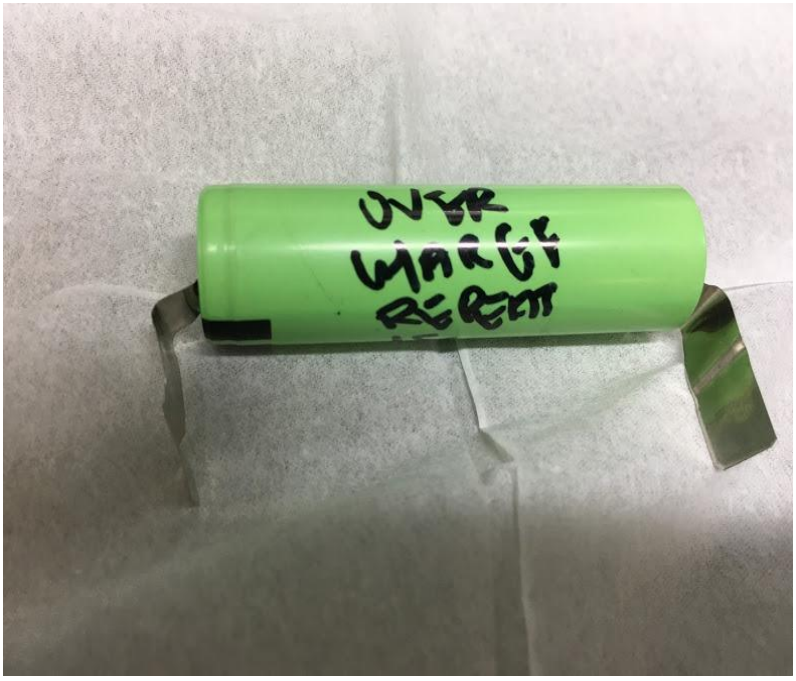

Figure 32 A Panasonic NCR18650B Li-ion cell that has been overcharged and is ready to be diassembled.

5. Removal of plastic cover – The external plastic cover of the cell is removed by making two small cuts with a scalpel on either the top or the bottom surface. The cells can then be peeled either by hand or tweezers of choice.
6. Cutting of cell header – Once the metallic can and the cell header are exposed, the header can be cut from the body. A metallic can cutter is used for this.
7. Detachment of cell header – Once the cell header is loosened from the body, the only component attaching the cell header to the jelly roll is the positive tab. This tab is cut with a pair of scissors. Caution: Care must be taken to ensure that the metallic tips of the scissors do not touch the can as this can create a short circuit in the cell. The cell header is placed in one of the designated plastic bags for later disassembly. This can be done outside the glove box.

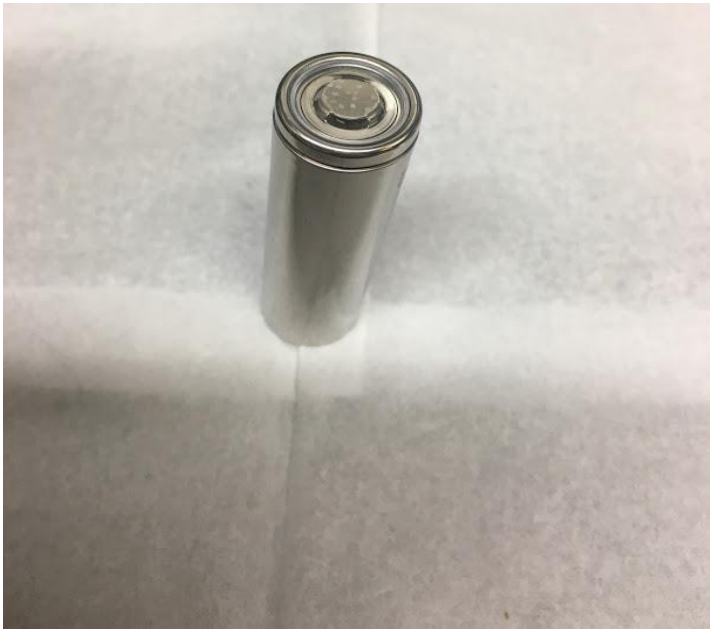

Figure 33 The stainless steel can and the cell header of the cell are exposed after removal of plastic wrapping.

8. Removal of can – Once the cell header is detached, the next step is to cut the metal can that houses the electrodes. Initially, cuts are made along the top of the cell via wide tipped pliers. With a pair of narrow tipped pliers, small strips of metal are peeled in a preferably spiral method which will allow easier removal. The strips of metal that are peeled are cut periodically as they may potentially cut through the experimenters gloves if they are allowed to become too long [Figure 34].
9. Removal of tape and tab – When the can is removed, it exposes the jelly roll of the electrodes as well as the negative tab bound together by tape. This tape is removed with a pair of narrow metallic tweezers and the tab is detached as well.

10. Separation of jelly roll – The electrodes and the separators wound together will now be clearly visible in the jelly roll configuration. These can be peeled apart for further visual inspection. Caution: While separating the electrodes, care must be taken to avoid contact between the anode and cathode as this can lead to a short circuit situation. Figure 36 shows the jelly roll arrangement of the electrodes
11. Inspection and storage – The electrodes and separators can now be separated, inspected, documented and kept for storage in their designated air tight containers.
12. All the tools required are shown in Figure 37.

Figure 34 The process of removal of the stainless steel can housing the jelly roll electrodes. Tops of the electrodes, some electrolyte and the cut positive tab are visible.

Figure 35 The tape that holds the electrodes together in the jelly roll configuration. A portion of the negetive tab that is attached to the anode is visible.

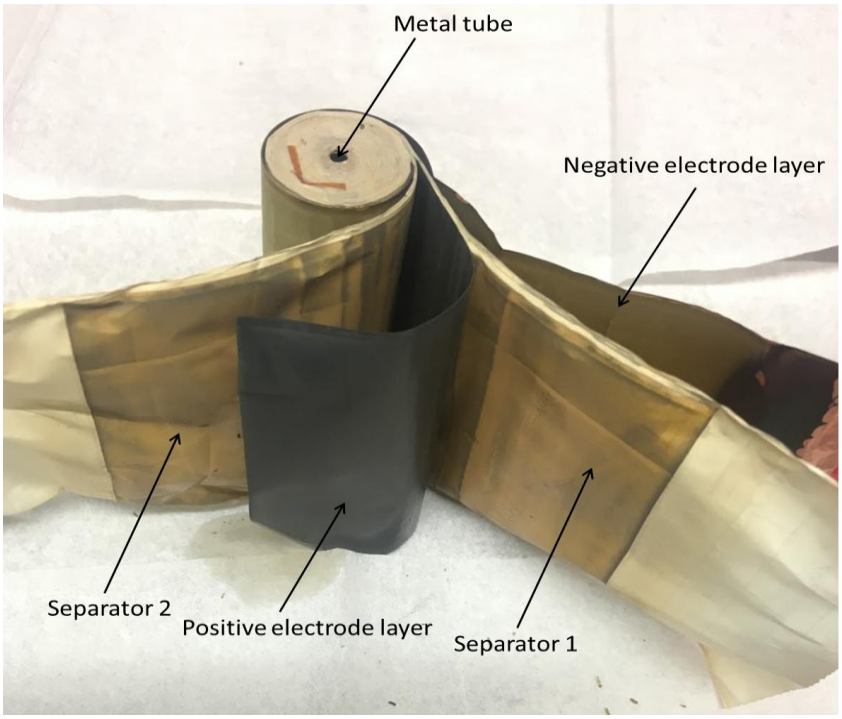

Figure 36 Jelly roll configuration of the Li-ion cylindrical cells. The anode and cathode separated by two separator layers are visible.

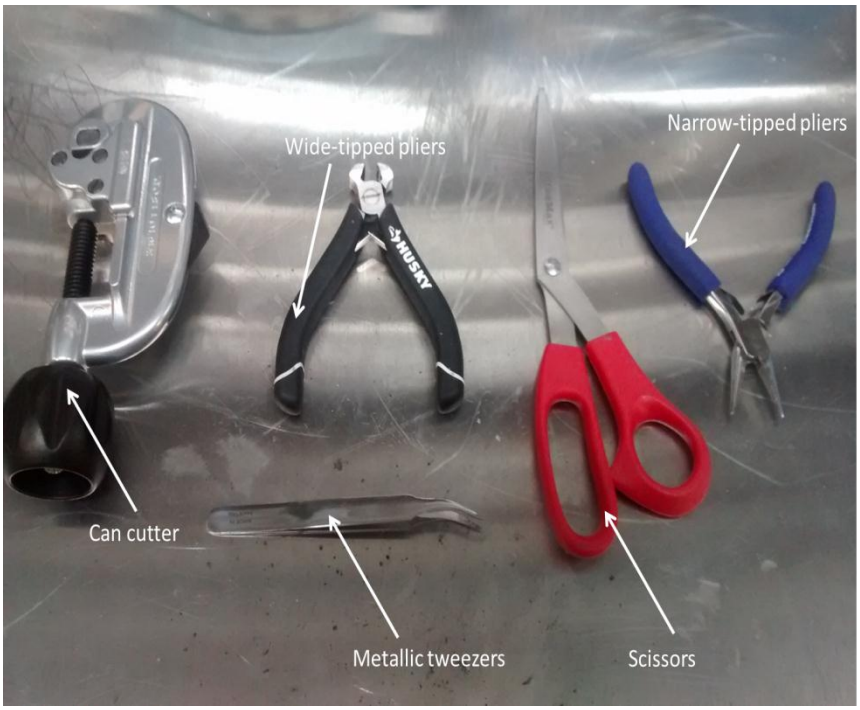

Figure 37 Tools that were used throughout the destructive physical analysis procedure of Panasonic Li-ion 18650 cells.

Effect of C-Rate

Cathodes

The destructive physical analysis enabled the visual inspection of the electrodes for the 18650 cells that were overcharged at various charging rates. Figure 38 shows the cathodes and corresponding separators retrieved from three cells overcharged at 1C, 2C, and 3C. The yellow tabs in the middle of the cathodes show the center of the electrode. The portion to the left of the tab shows the portion of the electrode that was at the center of the jelly roll and the portion on the right hand side shows the part of the cathode facing away from the center. Regardless of whether it is the anode or cathode, the electrodes always show more damage towards the center than at the other end. At a

glance, all three cathodes seem to have extensive cathode material delamination. Upon closer inspection, the cathode for 1C shows the highest amount of delamination. The cathode material in this cell has transferred heavily on to the separator. In the cells charged at 2C and 3C, there is definite delamination; however the transfer of materials onto the separator is lower.

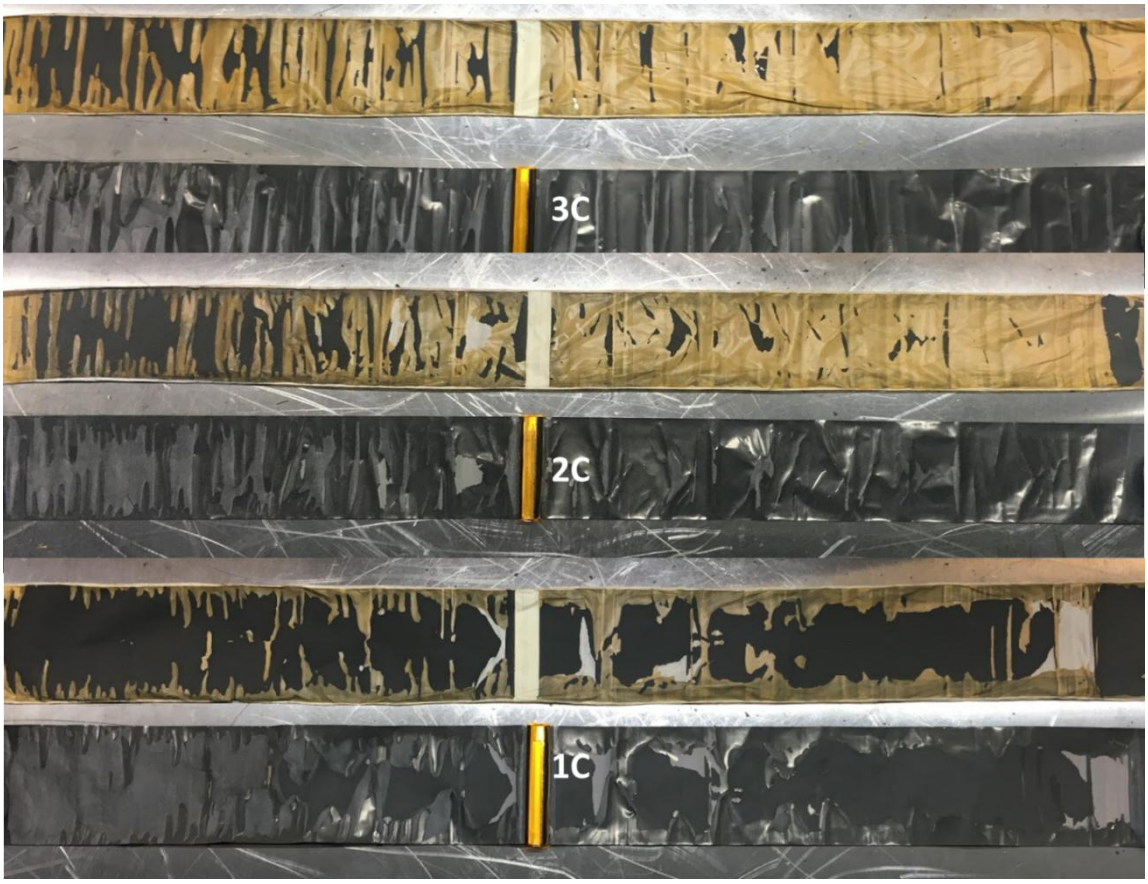

Figure 38 Visual inspection of the cathodes recovered from overcharged Li-ion cells at 1C, 2C, and 3C rates of charging.

Figure 39 show a similar cathode-separator layout for the cells charged at C/2, C/5 and C/10 charging rates. In the cells charged at C/10, C/5 and C/2, the amount of

delamination appears to be the same overall. At slow C-rates, the time taken by the cell to charge/overcharge is higher. This means that throughout the course of the test, any temperature rise occurring in the cell is able to dissipate better due to the longer charging time. Solid state diffusion transport of Li-ions in the cell is better enhanced at a higher temperature. Hence, if the temperature rise in the cell is low, the diffusion process is likely to be hindered as well, thereby preventing the full lithiation of the anode and rendering the cell to fail at a lower voltage.

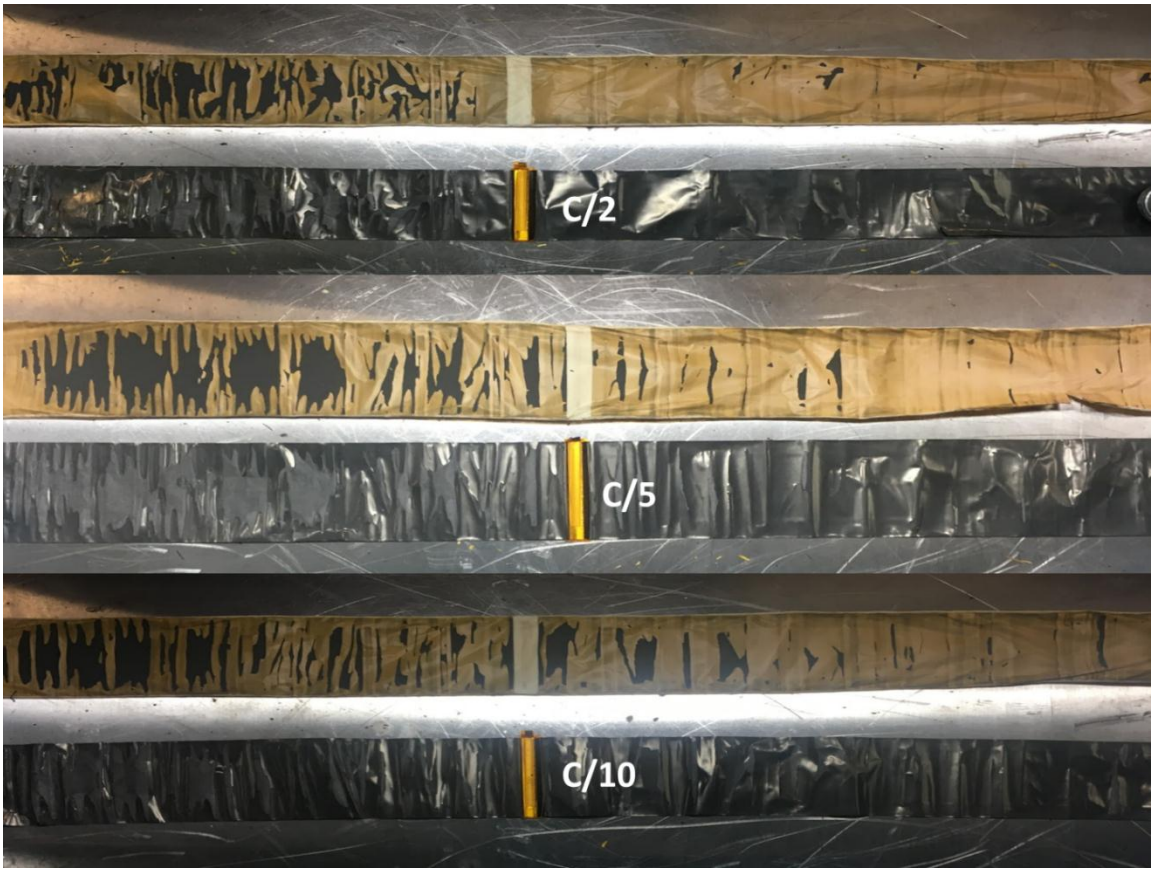

Figure 39 Visual inspection of the cathodes recovered from overcharged Li-ion cells at 0.1C,0.2C and 0.5C rates of charging.

Anodes

The anodes obtained after post-mortem analysis portray important results. Figure 40 shows the anodes retrieved from the cells after overcharging them at 0.1C, 0.2C, 0.5C, 1C, 2C and 3C rates. A cell that is fresh and hasn't been cycled at all will show an anode that is blackish grey in color. The anodes visible in the figure are a golden hue. This golden color is representative of a lithiated anode. The analysis will progress starting from the lowest C-rate. The anode obtained from the C/10 cell shows an almost uniform, completely lithiated anode with a small line in the middle of the anode that wasn't fully lithiated. There is no apparent plating to be noticed on this anode. The anode from the C/5 cell shows the presence of lithium plating in the form of greyish spots on the anode surface. Similarly, lithium plating is observed for both C/2 and 1C charged cells. Finally, at higher C-rates of 2C and 3C, there is no plating observed and greyish black areas representative of an unlithiated anode are visible. Recalling the cathode health of 0.1C, there was some transfer of cathode material to be found on the separator and correspondingly, there is a small area of the anode that wasn't able to receive lithium ions due to the cathode material having adhered on to separator instead of intercalating through it to the anode side. On the cathodes of cells charged at C/2, and C/5, there is very little transfer of cathode material onto the separator which means that most of the lithium was able to intercalate at least from the portion away from the center. Correspondingly, the anodes of these two cells show no signs of unlithiated anode and very visible signs of lithium plating. The cell charged at 1C shows extreme damage regardless of the side of the cathode. The anode also shows a significant amount of

lithium plating. In fact, the cathodes of this cell show certain whitish grey portions which indicate that the yellowish tinged ceramic coating that is usually applied to the separator has been degraded during overcharge. This is correlated to be the activation of the separator shutdown mechanism that is one of the ways that commercial cells are protected today. It is concluded that, the cathode of the cell charged at 1C had a higher stability as compared to the cathodes of cells charged at 2C and 3C. This can be derived from inspection of the cathodes as well as confirmation of these results from the voltage and temperature profiles of these cells. Since the cathodes of cells charged at 2C and 3C were not stable for long, these cathodes were unable to provide a continuous lithium inventory which could intercalate into the anode. Thus, the anodes from 2C and 3C show incomplete intercalation. Therefore, electrochemical cycling and destructive physical analyses are powerful tools that can aid in investigating the cross-talk between the electrodes during overcharge operation.

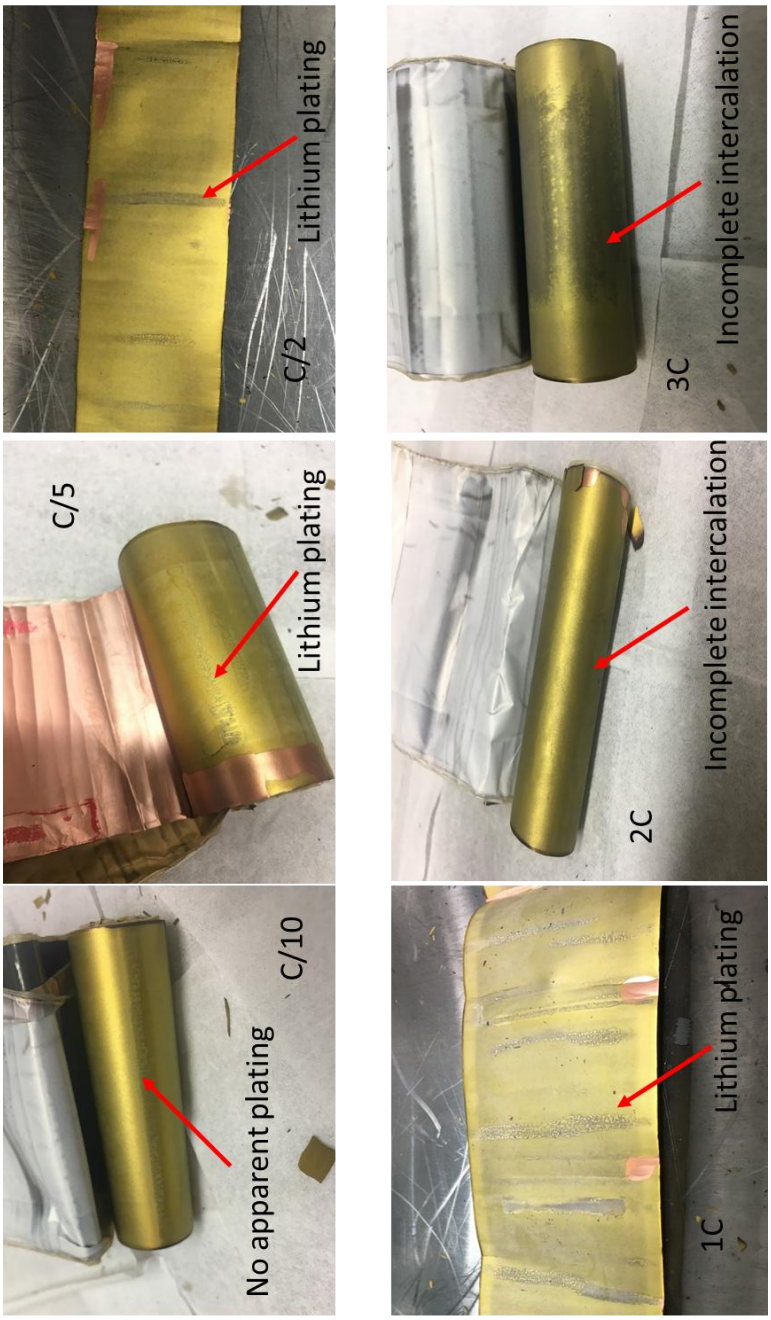

Figure 40 Anodes retrieved from Li -ion cells overcharge at 0.1C, 0.2C, 0.5C, 1C, 2C, and 3C charging rates.

CHAPTER V

CONCLUSIONS AND FUTURE WORK

In the present work, the safety degradation interaction of lithium-ion cells under overcharge abuse conditions was analyzed using experimental techniques. Before starting any experiment, a careful evaluation of the parameters of interest, and the information that is hoped to be gained must be performed. When previous works of overcharge of Li-ion cells are considered, it soon becomes apparent that there is very little structure, commonality or standard rules and practices that are in place for testing these cells. Hence, the first and foremost aim of this study was to implement two formation protocols and test three cells with each protocol in order to distinguish the advantages or disadvantages of using one or the other protocol. It was found that overcharging of Li-ion cells is path dependent. At the end of any test, the maximum voltage and temperatures achieved were the same regardless of the protocol used. However, the time taken for the cell to reach the end variables differed. Overall, no significant advantages or disadvantages were with use of either protocol. Secondly, in a set of tests where the electrochemical stability window of Li-ion cells was manipulated, the cycling tolerance of cells under overcharge was studied. When four lithium ion cells were charged to various cut off voltages – 4.2, 4.3, 4.4 and 4.5 (4.2 V being the safe upper limit), it was found that with an increase in upper voltage limit, higher capacity but a poorer cycling capability was obtained. This showed that even though there are alternative methods to achieving higher capacity from a Li-ion cell, dire effects on the safety and life of the cell may be seen. The next question that was answered in this work

is the effect of charging rate on the overcharge abuse behavior of a cylindrical Li-ion cell. It will reiterated one more time that overcharge is a behavior is that most heavily dependent on the cell chemistry than any other factor. This is also the reason commercial Panasonic cylindrical 18650 cells were the focus of this work. Because these cells are used heavily in the industry today, overcharge safety research on these cells would be directly beneficial and applicable in the industry. When the charging rate of three cells was varied to 0.1C, 1C and 2C, it was found that the cell charged at 1C failed at a voltage and temperature higher than the rest, followed by the 2C cell and finally, the C/10 cell. Upon first glance, this result may seem unexpected and erroneous. However, when these cells were opened during DPA, certain facts became clear. The cell charged at 1C had the most amount of cathode delamination and presence of lithium plating. It was inferred that this cathode was in fact, the most stable of the cathodes from the three cells. Since this cathode was able to withstand a higher voltage window, there was excess lithium that was able to intercalate from cathode to anode. This explains both the heavier delamination of the cathode and the lithium plating on the anode. The cell charged at 2C, failed at a similar voltage which was slightly lower than the first one. Upon visual inspection of its electrodes, it was seen that the cathode had less severe delamination and the anode had no presence of lithium plating. There were certain areas on the anode which hadn't been fully intercalated with lithium. The cathode of this cell was not as electrochemically stable in the voltage window between 4.2-5.13 V due to the higher charging rate. Hence, the cathode and eventually, the cell, failed quickly before the cathode could provide enough lithium repository for a full lithium intercalation.

Lastly, electrochemical impedance studies done on a Li-ion cell overcharged at C/25 were analyzed. These results indicated that in the overcharge region, there was a rise in separator resistance with the progression of overcharge up to failure. A separator shutdown occurs because the pores of the separator start to close preventing the passage of lithium ions. The cause for the activation of the protection mechanisms in the cell is believed to be due to the cathode instability. Since the overcharge of this cell lasts for a longer time – approximately five hours, the cathode may not be able to withstand the abuse conditions for such a long period and hence, the cell fails at a lower voltage. Similarly, since the overcharge of this cell lasts the longest, the cell is able to dissipate heat better than the other two cells which is why a lower temperature is seen in the cell.

Overcharge is often perceived as an anode centric phenomenon. By looking at the voltage and temperature behavior of the cell and corroborating the results with DPA results, it is seen that overcharge is rather a cathode-centric phenomenon that is profoundly dependent on the charging rate in combination with the upper voltage limit of the cell.

For further research, the electrodes obtained during DPA will be analyzed more thoroughly via Scanning Electron Microscopy. Visual inspection of the components in a failed cell can only provide a limited amount of information. In order to gain confirmation of phenomena such as lithium plating, SEM images can prove to be a valuable tool. Furthermore, phenomena such as gas evolution may be further explored by performing gas chromatography tests.

REFERENCES

1. U.S. Energy Information Administration, *International Energy Outlook 2016*, in *International Energy Agency*. 2016. p. 1-276
2. Badwal, S.P., et al., *Emerging electrochemical energy conversion and storage technologies.* Front Chem, 2014. **2**: p. 79.
3. Rahn, C.D. and C.-Y. Wang, *Introduction*, in *Battery Systems Engineering*. 2013, John Wiley & Sons Ltd. p. 1-10.
4. Gavrilovic, T. *The Impact of Electric Vehicles on the Grid: Customer Adoption, Grid Load and Outlook*. 2016 [cited 2017 February 25th]; Available from: https://www.greentechmedia.com/research/report/the-impact-of-electric-vehicles-on-the-grid.
5. Pinkwart, K. and J. Tübke, *Thermodynamics and Mechanistics*, in *Handbook of Battery Materials*. 2011, Wiley-VCH Verlag GmbH & Co. KGaA. p. 1-26.
6. Doughty, D.H., *Battery Safety and Abuse Tolerance*, in *Handbook of Battery Materials*. 2011, Wiley-VCH Verlag GmbH & Co. KGaA. p. 905-938.
7. Gores, H.J., et al., *Liquid Nonaqueous Electrolytes*, in *Handbook of Battery Materials*. 2011, Wiley-VCH Verlag GmbH & Co. KGaA. p. 525-626.
8. Ye, J.N., et al., *Thermal behavior and failure mechanism of lithium ion cells during overcharge under adiabatic conditions.* Applied Energy, 2016. **182**: p. 464-474.
9. Liu, Z., W. Fu, and C. Liang, *Lithium–Sulfur Batteries*, in *Handbook of Battery Materials*. 2011, Wiley-VCH Verlag GmbH & Co. KGaA. p. 811-840.

10. Larsson, F. and B.E. Mellander, *Abuse by External Heating, Overcharge and Short Circuiting of Commercial Lithium-Ion Battery Cells.* Journal of the Electrochemical Society, 2014. **161**(10): p. A1611-A1617.

11. Bandhauer, T.M., S. Garimella, and T.F. Fuller, *A critical review of thermal issues in lithium-ion batteries.* Journal of the Electrochemical Society, 2011. **158**(3): p. R1-R25.

12. Spotnitz, R. and J. Franklin, *Abuse behavior of high-power, lithium-ion cells.* Journal of Power Sources, 2003. **113**(1): p. 81-100.

13. Verma, P., P. Maire, and P. Novak, *A review of the features and analyses of the solid electrolyte interphase in Li-ion batteries.* Electrochimica Acta, 2010. **55**(22): p. 6332-6341.

14. Lisbona, D. and T. Snee, *A review of hazards associated with primary lithium and lithium-ion batteries.* Process Safety and Environmental Protection, 2011. **89**(6): p. 434-442.

15. Garcia, M., et al., *Instability of Polyvinylidene Fluoride-Based Polymeric Binder in Lithium-Ion Cells: Final Report*. 1999, ; Sandia National Labs., Albuquerque, NM (US); Sandia National Labs., Livermore, CA (US). p. Medium: P; Size: 43 pages.

16. Richard, M.N. and J.R. Dahn, *Accelerating rate calorimetry study on the thermal stability of lithium intercalated graphite in electrolyte I. Experimental.* Journal of the Electrochemical Society, 1999. **146**(6): p. 2068-2077.

17. Biensan, P., et al., *On safety of lithium-ion cells.* Journal of Power Sources, 1999. **81**: p. 906-912.

18. Buqa, H., et al., *Study of styrene butadiene rubber and sodium methyl cellulose as binder for negative electrodes in lithium-ion batteries.* Journal of Power Sources, 2006. **161**(1): p. 617-622.

19. Maleki, H., et al., *Thermal stability studies of Li-ion cells and components.* Journal of the Electrochemical Society, 1999. **146**(9): p. 3224-3229.

20. Du Pasquier, A., et al., *Differential scanning calorimetry study of the reactivity of carbon anodes in plastic Li-ion batteries (vol 145, pg 473, 1998).* Journal of the Electrochemical Society, 1998. **145**(4): p. 1413-1413.

21. Feng, X.M., X.P. Ai, and H.X. Yang, *Possible use of methylbenzenes as electrolyte additives for improving the overcharge tolerances of Li-ion batteries.* Journal of Applied Electrochemistry, 2004. **34**(12): p. 1199-1203.

22. Leising, R.A., et al., *A study of the overcharge reaction of lithium-ion batteries.* Journal of Power Sources, 2001. **97-8**: p. 681-683.

23. Zhang, S.S., *A review on electrolyte additives for lithium-ion batteries.* Journal of Power Sources, 2006. **162**(2): p. 1379-1394.

24. Roth, E., D. Doughty, and D. Pile, *Effects of separator breakdown on abuse response of 18650 Li-ion cells.* Journal of Power Sources, 2007. **174**(2): p. 579-583.

25. Roth, E.P., *Abuse response of 18650 Li-ion cells with different cathodes using EC: EMC/LiPF6 and EC: PC: DMC/LiPF6 electrolytes.* ECS Transactions, 2008. **11**(19): p. 19-41.

26. Tobishima, S., et al., *Lithium ion cell safety.* Journal of Power Sources, 2000. **90**(2): p. 188-195.

27. Tobishima, S. and J. Yamaki, *A consideration of lithium cell safety.* Journal of Power Sources, 1999. **81**: p. 882-886.

28. Larsson, F., et al., *Characteristics of lithium-ion batteries during fire tests.* Journal of Power Sources, 2014. **271**: p. 414-420.

29. Sahraei, E., J. Campbell, and T. Wierzbicki, *Modeling and short circuit detection of 18650 Li-ion cells under mechanical abuse conditions.* Journal of Power Sources, 2012. **220**: p. 360-372.

30. Lamb, J. and C.J. Orendorff, *Evaluation of mechanical abuse techniques in lithium ion batteries.* Journal of Power Sources, 2014. **247**: p. 189-196.

31. Ichimura, M., *The safety characteristics of lithium-ion batteries for mobile phones and the nail penetration test.* Intelec 07 - 29th International Telecommunications Energy Conference, Vols 1 and 2, 2007: p. 687-692.

32. Chen, J., C. Buhrmester, and J.R. Dahn, *Chemical overcharge and overdischarge protection for lithium-ion batteries.* Electrochemical and Solid State Letters, 2005. **8**(1): p. A59-A62.

33. Chen, Z.H., Y. Qin, and K. Amine, *Redox shuttles for safer lithium-ion batteries.* Electrochimica Acta, 2009. **54**(24): p. 5605-5613.

34. Kaur, A.P., et al., *Overcharge protection of lithium-ion batteries above 4 V with a perfluorinated phenothiazine derivative.* Journal of Materials Chemistry A, 2016. **4**(15): p. 5410-5414.

35. Hagen, M., et al., *Lithium–Sulfur Cells: The Gap between the State-of-the-Art and the Requirements for High Energy Battery Cells.* Advanced Energy Materials, 2015. **5**(16).

36. Venugopal, G., *Characterization of thermal cut-off mechanisms in prismatic lithium-ion batteries.* Journal of Power Sources, 2001. **101**(2): p. 231-237.

37. Roth, E.P., D.H. Doughty, and D.L. Pile, *Effects of separator breakdown on abuse response of 18650 Li-ion cells.* Journal of Power Sources, 2007. **174**(2): p. 579-583.

38. Bro, B. *Battery Safety 101: Anatomy - PTC vs PCB vs CID*. 2015 [cited 2017 April 27]; Available from: https://batterybro.com/blogs/18650-wholesale-battery-reviews/18306003-battery-safety-101-anatomy-ptc-vs-pcb-vs-cid.

39. Balakrishnan, P.G., R. Ramesh, and T.P. Kumar, *Safety mechanisms in lithium-ion batteries.* Journal of Power Sources, 2006. **155**(2): p. 401-414.

40. Hossain, S., et al., *Overcharge studies of carbon fiber composite-based lithium-ion cells.* Journal of power sources, 2006. **161**(1): p. 640-647.

41. Finegan, D.P., et al., *Investigating lithium-ion battery materials during overcharge-induced thermal runaway: an operando and multi-scale X-ray CT study.* Physical Chemistry Chemical Physics, 2016. **18**(45): p. 30912-30919.

42. Lu, L.G., et al., *A review on the key issues for lithium-ion battery management in electric vehicles.* Journal of Power Sources, 2013. **226**: p. 272-288.

43. Mendoza-Hernandez, O.S., et al., *Cathode material comparison of thermal runaway behavior of Li-ion cells at different state of charges including over charge.* Journal of Power Sources, 2015. **280**: p. 499-504.

44. Xu, F., et al., *Failure Investigation of LiFePO4 Cells under Overcharge Conditions.* Journal of the Electrochemical Society, 2012. **159**(5): p. A678-A687.

45. Zhang, S.S., K. Xu, and T.R. Jow, *Electrochemical impedance study on the low temperature of Li-ion batteries.* Electrochimica Acta, 2004. **49**(7): p. 1057-1061.

46. Nishio, K. and N. Furukawa, *Practical Batteries*, in *Handbook of Battery Materials*. 2011, Wiley-VCH Verlag GmbH & Co. KGaA. p. 27-85.